NACA

RESEARCH MEMORANDUM

A TRANSONIC-WING INVESTIGATION IN THE LANGLEY 8-FOOT HIGH-SPEED TUNNEL AT HIGH SUBSONIC MACH NUMBERS AND AT A MACH NUMBER OF 1.2

WING-FUSELAGE CONFIGURATION HAVING A WING OF 60° SWEEPBACK, ASPECT RATIO 4, TAPER RATIO 0.6, AND NACA 65A006 AIRFOIL SECTION

By Raymond B. Wood and Frank F. Fleming

Langley Aeronautical Laboratory
Langley Field, Va.

NATIONAL ADVISORY COMMITTEE
FOR AERONAUTICS

WASHINGTON

January 24, 1951

[redacted]

NATIONAL ADVISORY COMMITTEE FOR AERONAUTICS

RESEARCH MEMORANDUM

A TRANSONIC-WING INVESTIGATION IN THE LANGLEY 8-FOOT HIGH-SPEED TUNNEL AT HIGH SUBSONIC MACH NUMBERS AND AT A MACH NUMBER OF 1.2

WING-FUSELAGE CONFIGURATION HAVING A WING OF 60° SWEEPBACK, ASPECT RATIO 4, TAPER RATIO 0.6, AND NACA 65A006 AIRFOIL SECTION

By Raymond B. Wood and Frank F. Fleming

SUMMARY

As part of the transonic-wing program the effect of sweep on wings employing the NACA 65A006 airfoil section was investigated in the Langley 8-foot high-speed tunnel. This paper presents the results of an investigation of a wing having this airfoil section, 60° of sweepback at the quarter chord, an aspect ratio of 4, and a taper ratio of 0.6.

Lift, drag, and pitching-moment data are presented for the basic wing-fuselage configuration and the wing with wing-fuselage interference for a Mach number range from 0.60 to 0.96 and for a Mach number of 1.2. No lift- or drag-force break was noted for the wing-fuselage configuration at subsonic Mach numbers although the pitching-moment curve did break at angles of attack greater than 8°. The maximum lift-drag ratio of the wing-fuselage combination did not decrease sharply at high subsonic Mach numbers, but the value of the maximum lift-drag ratio was decreased 40 percent from a Mach number of 0.96 to a Mach number of 1.2.

Undesirable pitching-moment characteristics as experienced by the wing-fuselage configuration (when the center-of-gravity position is located at 0.25 wing mean aerodynamic chord) exist at a lift coefficient of approximately 0.3. Qualitative calculations show that, at subsonic speeds in the lift-coefficient range from zero to 0.25, the aerodynamic-center location moved rearward 0.24 wing mean aerodynamic chord, followed by a rapid forward movement of 0.37 wing mean aerodynamic chord in the

[redacted]

[redacted]

lift-coefficient range from 0.25 to 0.4. By moving the center-of-gravity position forward, some of the undesirable pitching-moment characteristics may be avoided. However, the resultant stability at low lift coefficients might then present a difficult flight-control problem.

The downwash angle increased regularly as the angle of attack of the wing increased throughout the subsonic Mach number range. At a Mach number of 1.2, reversals in the rate of change of the downwash angle with the wing angle of attack occurred as the angle of attack increased and indicated that undesirable longitudinal-trim adjustments would be necessary for any airplane using this wing. These adverse characteristics may be present in the region between a Mach number of 0.96 and a Mach number of 1.2.

The probable tail-height location to be out of the wake would be approximately equal to 35 percent of the wing semispan.

INTRODUCTION

As part of a research program conducted by the National Advisory Committee for Aeronautics, a series of wing-fuselage configurations is being investigated in the Langley 8-foot high-speed tunnel to study the effects of wing geometry on the aerodynamic characteristics at transonic speeds.

This paper presents the results of an investigation of a wing-fuselage configuration having a wing with 60° sweepback referred to the quarter-chord line, an aspect ratio of 4, a taper ratio of 0.6, and an NACA 65A006 airfoil section measured parallel to the plane of symmetry.

For this investigation, lift, drag, and pitching-moment characteristics were determined at various angles of attack through a Mach number range from 0.60 to 0.96 and at a Mach number of 1.2. Downwash angles and wake characteristics were obtained at the rear of the model for two spanwise locations at three tail-height planes above the wing-chord plane.

This series of wings has also been tested on the transonic bump in the Langley high-speed 7- by 10-foot tunnel. A comparison of the results obtained by the transonic-bump technique and the results obtained at the Langley 8-foot high-speed tunnel (sting-support technique) is presented in reference 1.

SYMBOLS

A	aspect ratio
λ	taper ratio
C_D	drag coefficient $\left(\frac{D}{qS}\right)$
C_L	lift coefficient $\left(\frac{L}{qS}\right)$
C_m	pitching-moment coefficient $\left(\frac{M_{\bar{c}/4}}{qS\bar{c}}\right)$
$\bar{c}$	wing mean aerodynamic chord, inches
D	drag, pounds
H	total-pressure loss in the wake, pounds per square foot
l	fuselage basic body length, inches
L	lift, pounds
M	Mach number
$M_{\bar{c}/4}$	pitching moment about the quarter chord, inch-pounds
P_b	base-pressure coefficient $\left(\frac{p_b - p_o}{q}\right)$
p_b	static pressure at the rear of the model, pounds per square foot
p_o	free-stream static pressure, pounds per square foot
q	free-stream dynamic pressure, pounds per square foot, $\left(\frac{1}{2}\rho V^2\right)$
r	fuselage radius at station x, inches
R	Reynolds number (based on $\bar{c}$ expressed in feet)
S	wing area, square feet
V	free-stream velocity, feet per second

x	longitudinal distance from the nose of the body, inches
α	angle of attack, degrees
ϵ	downwash angle, degrees
ρ	free-stream density, slugs per cubic foot
$\frac{\Delta\alpha}{L/S}$	change of angle of attack for given lift loads due to bending

APPARATUS AND METHODS

Tunnel.- The investigation was conducted in the Langley 8-foot high-speed tunnel. Test sections for both subsonic-flow and supersonic-flow regions were provided by means of a plaster liner installed on the tunnel wall. Calibration tests have shown an essentially constant velocity in the subsonic test section within the accuracy of the calibration technique up to the highest subsonic test Mach number. The maximum deviation from the design Mach number 1.2 in the supersonic test region was 0.02 (reference 2).

Model.- The fuselage, a steel body of revolution with a fineness ratio of 12, was shortened to an effective fineness ratio of 10 so that the body could be mounted on a sting-support system. The wing used in this investigation was an aluminum wing swept back 60° at the quarter-chord line, with a taper ratio of 0.6, an aspect ratio of 4.0, and an NACA 65A006 airfoil section measured parallel to the air stream. Dimensions of the wing and fuselage, as well as the location of the midwing installation relative to the fuselage longitudinal axis, are shown in figure 1.

Tests.- The model was mounted in the tunnel on an extensible sting-support system, which enabled the model to be placed in either the subsonic-flow or supersonic-flow region by moving the support system longitudinally. The location of the model in both flow regions is shown in figure 2. During subsonic testing, static pressures were observed along the tunnel wall in the region of the model location to insure that no data were obtained that would be influenced by the tunnel-choking phenomenon. For testing at a Mach number of 1.2, shadow images of the tunnel normal shock were observed to insure that test data were not taken with the normal shock on the model.

The angle of attack of the model was varied through the Mach number range by means of a remote-control mechanism. Measurements of the angle

of attack were accomplished by means of a simple optical system. A description of the angle-of-attack apparatus can be found in reference 3.

Point downwash measurements were obtained from rakes mounted behind the model at two spanwise locations. A sketch showing the rake locations relative to the fuselage can be seen in figure 3.

A close-up photograph of the model, the support system, rakes, and the mirror used for the optical measuring system is shown in figure 4.

The fuselage alone was tested in a previous investigation at various angles of attack for a subsonic Mach number range from 0.60 to 0.96 and for a supersonic Mach number of 1.2. The aerodynamic characteristics for the fuselage-alone configuration are not presented in this paper but can be found in reference 3. The wing-fuselage combination considered in this investigation was tested through a Mach number range similar to that of the fuselage-alone configuration. Data are presented for the wing-fuselage and for the wing with wing-fuselage interference.

A transition strip was installed on the wing and the fuselage in order that an approximation of the nature of the flow over the wing-fuselage configuration at higher Reynolds numbers could be obtained. Data are presented for the wing-fuselage combination with the transition strip installed at the 10-percent chord line on both the upper and lower surfaces of the wing and approximately 10 percent of the fuselage length behind the fuselage nose. The transition strips were about 0.125 inch wide and consisted of No. 60 carborundum grains imbedded in a clear adhesive substance on the wing and fuselage.

The accuracy of the C_L, C_D, and C_m measurements is 0.010, 0.001, and 0.005, respectively. The error in measuring the angle of attack was found to a maximum of 0.10°.

CORRECTIONS AND COMPUTATIONS

Wind-tunnel-wall corrections.- By using the methods outlined in reference 4 (straight wings) and an approximate method of reference 2 (swept wings) corrections for tunnel blockage were applied to the Mach number. The dynamic pressure and Reynolds number corrections were small, and the Mach number corrections varied from 0.7 percent at $M = 0.85$ to 1.5 percent at $M = 0.96$. Figure 5 shows the variation of test Reynolds number with Mach number. The drag corrections were negligible at all Mach numbers except $M = 0.96$ where the applied correction amounted to about 2 percent (reference 4).

By the method described in reference 5, jet-boundary induced-upwash corrections were calculated. However, these corrections were considered negligible for the lift, drag, and pitching-moment coefficients when the maximum corrections were found to be less than 1 percent. Downwash-angle corrections were not obtained directly but were obtained by extrapolation from a curve given in reference 4 for the variation of the downwash-angle corrections with sweep angle. These corrections were applied to the data throughout the subsonic Mach number range tested. At the highest angle of attack, the maximum downwash-angle correction was 0.2°.

Corrections for bow-wave loss were applied to the total-pressure-loss coefficient $\frac{\Delta H}{q}$ at $M = 1.2$.

Wing-fuselage interference.- As previously mentioned, data are presented for the wing-fuselage combination and for the wing and wing-fuselage interference. Data were obtained for the second condition by subtracting the fuselage-alone data from the wing-fuselage-combination data. The force and moment coefficients for the wing with wing-fuselage interference are, of course, based on the total wing area including that part covered by the fuselage. Unfortunately, wing-alone characteristics cannot be inferred from the wing and wing-fuselage-interference data because of a lack of information on wing-fuselage interference at high Mach numbers. Some qualitative indications of the nature of the differences in wing-alone data and wing-with-wing-fuselage-interference data at high Mach numbers can perhaps be obtained from a study of the low-speed investigation of wing-fuselage interference described in reference 6. The data of reference 6 indicated the following differences in the force and moment coefficients could be expected in comparing wing-alone data and wing-with-wing-fuselage-interference data:

Drag - The drag values of the wing with wing-fuselage interference will be lower than the drag values of a wing-alone configuration since the data for the wing with wing-fuselage interference in order to be comparable would have to be calculated based on the exposed wing area (wing-fuselage configuration) rather than the complete wing area.

Lift - The value of C_L (wing and wing-fuselage interference) is expected to be higher than C_L (wing-alone) since the fuselage in a wing-fuselage combination is capable of carrying more lift than as a fuselage alone.

Pitching moment - The C_m values will be more negative for the wing with wing-fuselage interference than for the C_m of a

wing alone. This condition would be expected since the center of pressure of the fuselage when installed in conjunction with the wing changes the loading on the wing causing a rearward shift of the wing center-of-pressure data.

Because of the lack of quantitative data on wing-fuselage interference at high Mach numbers, however, no attempt has been made to reduce the wing-and-wing-fuselage-interference data to wing-alone data. In spite of the lack of an exact interpretation, these data of the wing-and-wing-fuselage-interference are thought to be of interest since it seems reasonable that slight changes in fuselage length or diameter will not materially change the results obtained by subtracting fuselage-alone data from wing-fuselage-combination data. Thus, a designer could, perhaps, test the fuselage being considered and, by adding the fuselage-alone characteristics to those of the wing- and wing-fuselage interference data presented herein, obtain a reasonable value for a wing-fuselage combination.

Sting-support interference.- The presence of the sting at the rear of the fuselage would be expected to alter the static pressure in this region and, consequently, the measured characteristics of the complete model. Previous data obtained from reference 7 indicated that the sting-interference-tare values are negligible for the lift and pitching-moment coefficients. An interpolation of the results from the aforementioned reference indicated that the drag coefficients of the present model would be increased by the order of 0.003 at subsonic Mach numbers and 0.002 at a Mach number of 1.2. Sting-interference tares have been applied to the drag coefficient in the analysis plots. Therefore, these corrected values of the drag coefficient represent the free-flight drag coefficient. (Power off and all air ducts closed.) Sting-interference tares evaluated in reference 7 for base pressure coefficient indicate that the maximum corrections would be 0.10 for low angles of attack. The effect of the sting support on downwash-angle measurements from reference 7 indicated that a maximum error of 1.0° could be expected at subsonic Mach numbers and an error 0.2° at a Mach number of 1.2. However, these base-pressure and downwash corrections were not applied since the results were based on a very limited angle-of-attack range (-2° to $+4^\circ$).

Downwash calculations.- Downwash-angle calculations were made assuming the static pressure at the rake was equal to the free-stream static pressure.

The small inaccuracies occurring due to this assumption, errors in reading the manometer tubes, and the methods of measuring the rake angles constitute inaccuracy of $\pm 0.2^\circ$ except in the wake where the error may be increased to as much as $\pm 0.3^\circ$.

Base pressure.- Model base pressures were measured for all tests. The variation of base-pressure coefficient with Mach number is presented for various angles of attack for the wing-fuselage configuration in figure 6. By applying the base-pressure data to the basic wing-fuselage configuration, the conditions at the base of the model can be altered to represent free-stream conditons with the sting in place.

Effect of wing deflection.- Since an aluminum wing was used in the present investigation, the bending of the wing due to lift loads was considered for the wing-fuselage configuration. Theoretical span-load calculations were made by the methods described in references 8 and 9. The magnitude of the wing deflection and the change in the angle of attack due to wing deflection were calculated by assuming an elliptical span-load distribution. Static-load tests were then made to verify the calculated values since the moment of inertia at some wing sections was not easily determined. The rigid-wing computations were limited to $C_L \approx 0.4$ since the critical Mach number was attained. Beyond the critical Mach number, the basic assumptions of elliptical load distribution no longer apply. Estimations of the critical Mach number were based on two-dimensional-airfoil data. Then, by estimating that the elastic axis of the wing was at the 40-percent-chord line, the static-load tests were made. The change in angle of attack due to wing bending under static loads is shown in figure 7(a). By applying these results and the theoretical calculations, the aerodynamic effect of wing bending at a typical high Mach number was estimated (fig. 7(b)). The bending of the wing at zero lift shifted the aerodynamic-center location forward approximately 8 percent, and, at $C_L \approx 0.4$, the aerodynamic-center locations were shifted forward approximately 7 percent. Also, a decrease of approximately 7 percent in the slope of the lift curve was noted for the test data (flexible wing) as compared with the computed rigid-wing data.

After completing the investigation of wing bending about the assumed elastic axis, the wing was then statically loaded at the 25-percent-chord line to ascertain the effect of wing bending on the load parameter $\frac{\Delta\alpha}{L/S}$ if the wing loads were applied farther forward. The static-test results indicated that the $\frac{\Delta\alpha}{L/S}$ values would be decreased by 25 percent. Thus, in presenting these qualitative results in aerodynamic-coefficient form, it was thought that the worst condition of wing bending could be approximated. In the present investigation, the test data were not corrected for wing bending since sufficient data were not available at this time.

RESULTS AND DISCUSSION

A table of figures showing the results obtained in this investigation follows:

Force and Moment Characteristics

The variation of the lift, drag, and pitching moment with Mach number for the wing-fuselage configuration is shown in figure 8. There was no indication of a lift- or drag-force break at subsonic Mach numbers although the pitching-moment-coefficient curve did break at an angle of attack of 8°. As the angle of attack was further increased, the break in the pitching-moment curve occurred at lower Mach numbers. The effect of fixed transition on the wing-fuselage configuration (fig. 8) was rather small at all angles of attack except at 0°. At $\alpha = 0^\circ$, the fixed transition caused a drag rise of approximately 0.005 for all subsonic Mach numbers and at $M = 1.2$.

Figure 9 shows the comparison of data for the basic wing-fuselage configuration and the wing with wing-fuselage interference.

Lift.- The variation of lift with angle of attack (fig. 9(a)) showed very slight differences between the data for the wing-fuselage and the wing with wing-fuselage interference for all speeds at low lift coefficients. These differences can readily be seen in figure 10 by the comparison of the slopes of the lift curves for these data at zero lift. However, at higher lift coefficients (that is, $C_L = 0.4$) a comparison of these data showed that the slope of the lift curve for the wing with wing-fuselage interference is 10 percent lower than the basic wing-fuselage configuration (fig. 10).

Drag.- A comparison of the drag data for the wing-fuselage and the wing with wing-fuselage interference is shown in figure 9(b). Very low values of the minimum drag coefficient were noted for the wing with wing-fuselage interference. The variation of drag coefficient at zero lift with Mach number is shown in figure 11. Sting-interference tares have been applied to the drag data of the wing-fuselage configuration. The low values of the drag coefficient for the wing with wing-fuselage interference can be expected for reasons previously explained.

The maximum lift-drag ratio variation with Mach number for the wing-fuselage configuration is shown in figure 12. The drag values have been corrected for sting-interference effects. A decrease of approximately 8 percent in the maximum lift-drag value for the wing-fuselage configuration was noted from $M = 0.70$ to $M = 0.96$. This decrease is definitely in contrast with the sharp decrease in maximum lift-drag ratios at high subsonic Mach numbers for the wings of references 2 and 8. However, the trend of the maximum lift-drag ratio indicated that a 40-percent decrease can be expected between $M = 0.96$ and $M = 1.2$ for this wing. Similar decreases were noted for the wing of references 3 and 10.

Pitching moment.- The variation of pitching-moment coefficient with lift coefficient is shown in figure 9(c) for the wing-fuselage configuration and in figure 9(d) for the wing with wing-fuselage interference. The indications from figures 9(c) and 9(d) are that very undesirable pitching-moment characteristics exist around $C_L \approx 0.3$. This condition is brought out clearly in the comparison of the slopes of the pitching-moment curve $\frac{\partial C_m}{\partial C_L}$ in figure 13. To illustrate the effect of the unstable trends as experienced by this model (when the center-of-gravity position is located at $0.25\bar{c}$), a table of the movement of the average measured aerodynamic-center locations (through the subsonic Mach number range) is presented for three lift coefficients as follows:

Configuration	M	Aerodynamic-center location (percent $\bar{c}$)		
		$C_L = 0$	$C_L = 0.25$	$C_L = 0.4$
Wing-fuselage	0.60 to 0.96	19	43	6
	1.2	30	25	30
Wing and wing-fuselage interference	0.60 to 0.96	31	46	14
	1.2	43	35	0

It is of interest to note the behavior of the aerodynamic-center characteristics of the wing-fuselage configuration. At subsonic speeds in the lift-coefficient range from 0 to 0.25, the aerodynamic-center location moved rearward $0.24\bar{c}$ followed by a rapid forward movement of $0.37\bar{c}$ in the lift-coefficient range from 0.25 to 0.4.

On the basis of these qualitative data, it would seem that this wing would not be considered a good choice for a transonic airplane although, by moving the center-of-gravity position forward, some of the undesirable pitching-moment characteristics may be avoided. However, the designer should bear in mind that the resultant stability at very low lift coefficients might then be of such a nature as to make flight control very difficult.

Since the irregular and undesirable pitching characteristics shown in these results are applicable for low test Reynolds numbers, it may be thought that at higher Reynolds numbers the data would be altered. The low-speed tests of reference 11, however, indicate that even at higher Reynolds numbers ($R \leq 4.5 \times 10^6$) the undesirable pitching-moment phenomena also found in the present data would still have to be considered.

Wake and Downwash Characteristics

For the transonic-wing program, the 25-percent position of the mean aerodynamic chord was at the same location relative to the fuselage nose for all the wings tested. The two wake rakes used were located at two wing-semispan locations (8.3 and 29.2 percent). The extent of the wake was studied for all angles of attack (up to a Mach number of 0.93). Data are presented for only the basic wing-fuselage

configuration for angles of $\alpha \geq 4^\circ$ since the smaller angles indicated no appreciable wake size. Data are not presented at $M = 0.96$ because of tunnel-choking phenomena at angles of attack greater than 8°. The effects of wing deflection and Reynolds number upon the wake measurements were not evaluated.

The inboard rake (8.3-percent semispan location) showed very high pressure-loss peaks and a wide wake as shown in figure 14. Unpublished data obtained in the Langley 8-foot high-speed tunnel indicate that these phenomena are due to fuselage boundary-layer disturbances, weak shocks reflecting from the rear of the fuselage, and the presence of the sting. Measurements indicated that the width of the wake was much smaller at the outboard rake stations than for the inboard station so that the interference effect previously mentioned was greatly reduced. The data of figure 14 indicate that the position of a horizontal tail to be outside the wake should be approximately 35 percent of the wing semispan above the wing-chord plane.

At $M = 1.2$, the flow did not break away at $\alpha = 8^\circ$ but showed a tendency to do so at $\alpha = 10^\circ$. However, the tunnel normal shock was observed on the rear section of the model at $\alpha = 10^\circ$, but the data were thought to be of interest inasmuch as they show the general trend of the wake at a high angle of attack.

Downwash angles were measured at two wing-semispan locations (8.3 and 29.2 percent) for three tail-height positions (heights equal to 12.5, 25.0, and 37.5 percent wing semispan) above the wing-chord plane. The distance from the quarter-chord location of the mean aerodynamic chord to the rake was 1.225 wing semispans. The variation of downwash angle with wing angle of attack for all test Mach numbers is shown in figure 15 for both the wing-fuselage and the wing with wing-fuselage interference. The downwash angle increased regularly as the angle of attack of the wing increased throughout the subsonic Mach number range. At $M = 1.2$, reversals in the rate of change of the downwash angle with the wing angle of attack occurred as the angle of attack increased and indicated that undesirable longitudinal-trim adjustments would be necessary for any airplane using this wing. These adverse characteristics may be present in the region between $M = 0.96$ and $M = 1.2$.

From the wake survey (fig. 14) it was evident that the probable tail location (to be outside the wake) would be at a tail height approximately equal to 35 percent wing semispan above the wing-chord plane. Since data are available at a tail height of 37.5 percent wing semispan, the variation of the slope of the downwash curve with Mach number is presented for this location at two lift coefficients (fig. 16). The average values of $\frac{\partial \epsilon}{\partial \alpha}$ for $C_L = 0$ at both rake locations for the

chosen tail height (37.5 percent wing semispan) were approximately equal. At $C_L = 0.4$, the magnitude of the downwash angles measured at the outboard stations, however, were higher than those measured at the inboard station. For the chosen tail-height position, the slope of the downwash curve for the wing with wing-fuselage interference was higher at the outboard rake location than for the wing-fuselage configuration (fig. 16). This height can be attributed to a change in the direction of the angle of downwash for the fuselage-alone configuration at the higher angles of attack as measured at the outboard rake location.

CONCLUSIONS

From the investigation of the aerodynamic characteristics of the wing with 60° sweepback, an aspect ratio 4, a taper ratio 0.6, and an NACA 65A006 airfoil section, the following conclusions are made:

1. No lift- or drag-force break was noted for the wing-fuselage configuration at subsonic Mach numbers. The pitching-moment curve, however, did break at angles of attack greater than 8° and, as the angle of attack further increased, the pitching-moment break occurred at successively lower Mach numbers.

2. The maximum lift-drag ratio of the wing-fuselage combination did not decrease sharply at high subsonic Mach numbers, but the value of the maximum lift-drag ratio was decreased 40 percent from a Mach number of 0.96 to a Mach number of 1.2.

3. Undesirable pitching-moment characteristics as experienced by the model (when the center-of-gravity position is located at 0.25 wing mean aerodynamic chord) exist at a lift coefficient of approximately 0.3. Qualitative calculations show that, at subsonic speeds in the lift-coefficient range from zero to 0.25, the aerodynamic-center location moved rearward 0.24 wing mean aerodynamic chord followed by a rapid forward movement of 0.37 wing mean aerodynamic chord in the lift-coefficient range from 0.25 to 0.4. By moving the center-of-gravity position forward, some of the undesirable pitching-moment characteristics might be avoided. The resultant stability at very low lift coefficients, however, might then present a difficult flight-control problem.

4. The downwash angle increased regularly as the angle of attack of the wing increased throughout the subsonic Mach number range. At a Mach number of 1.2, reversals in the rate of change of the downwash angle with the wing angle of attack occurred as the angle of attack increased and indicated that undesirable longitudinal-trim adjustments

would be necessary for any airplane using this wing. These adverse characteristics may be present in the region between a Mach number of 0.96 and a Mach number of 1.2.

5. The probable tail-height location to be out of the wake would be approximately equal to 35 percent of the wing semispan.

Langley Aeronautical Laboratory
National Advisory Committee for Aeronautics
Langley Field, Va.

REFERENCES

1. Donlan, Charles J., Myers, Boyd C., II, and Mattson, Axel T.: A Comparison of the Aerodynamic Characteristics at Transonic Speeds of Four Wing-Fuselage Configurations as Determined from Different Test Techniques. NACA RM L50H02, 1950.

2. Ritchie, Virgil S., Wright, Ray H., and Tulin, Marshall P.: An 8-Foot Axisymmetrical Fixed Nozzle for Subsonic Mach Numbers up to 0.99 and for a Supersonic Mach Number of 1.2. NACA RM L50A03a, 1950.

3. Osborne, Robert S.: A Transonic-Wing Investigation in the Langley 8-Foot High-Speed Tunnel at High Subsonic Mach Numbers and at a Mach Number of 1.2. Wing-Fuselage Configuration with a Wing of 45° Sweepback, Aspect Ratio 4, Taper Ratio 0.6, and NACA 65A006 Airfoil Section. NACA RM L50H08, 1950.

4. Herriot, John G.: Blockage Corrections for Three-Dimensional-Flow Closed-Throat Wind Tunnels, with Consideration of the Effect of Compressibility. NACA RM A7B28, 1947.

5. Eisenstadt, Bertram J.: Boundary-Induced Upwash for Yawed and Swept-Back Wings in Closed Circular Wind Tunnels. NACA TN 1265, 1947.

6. Jacobs, Eastman N., and Ward, Kenneth E.: Interference of Wing and Fuselage from Tests of 209 Combinations in the N.A.C.A. Variable-Density Tunnel. NACA Rep. 540, 1935.

7. Osborne, Robert S.: High-Speed Wind-Tunnel Investigation of the Longitudinal Stability and Control Characteristics of a $\frac{1}{16}$-Scale Model of the D-558-2 Research Airplane at High Subsonic Mach Numbers and at a Mach Number of 1.2. NACA RM L9C04, 1949.

8. DeYoung, John: Theoretical Additional Span Loading Characteristics of Wings with Arbitrary Sweep, Aspect Ratio, and Taper Ratio. NACA TN 1491, 1947.

9. Diederich, Franklin W.: A Simple Approximate Method for Obtaining Spanwise Lift Distributions over Swept Wings. NACA RM L7I07, 1948.

[redacted]

10. Henry, Beverly Z., Jr.: A Transonic Wing Investigation in the Langley 8-Foot High-Speed Tunnel at High Subsonic Mach Numbers and at a Mach Number of 1.2. Wing-Fuselage Configuration Having a Wing of 35° Sweepback, Aspect Ratio 4, Taper Ratio 0.6, and NACA 65A006 Airfoil Section. NACA RM L50J09, 1950.

11. Cahill, Jones F., and Gottlieb, Stanley M.: Low-Speed Aerodynamic Characteristics of a Series of Swept Wings Having NACA 65A006 Airfoil Sections. NACA RM L50F16, 1950.

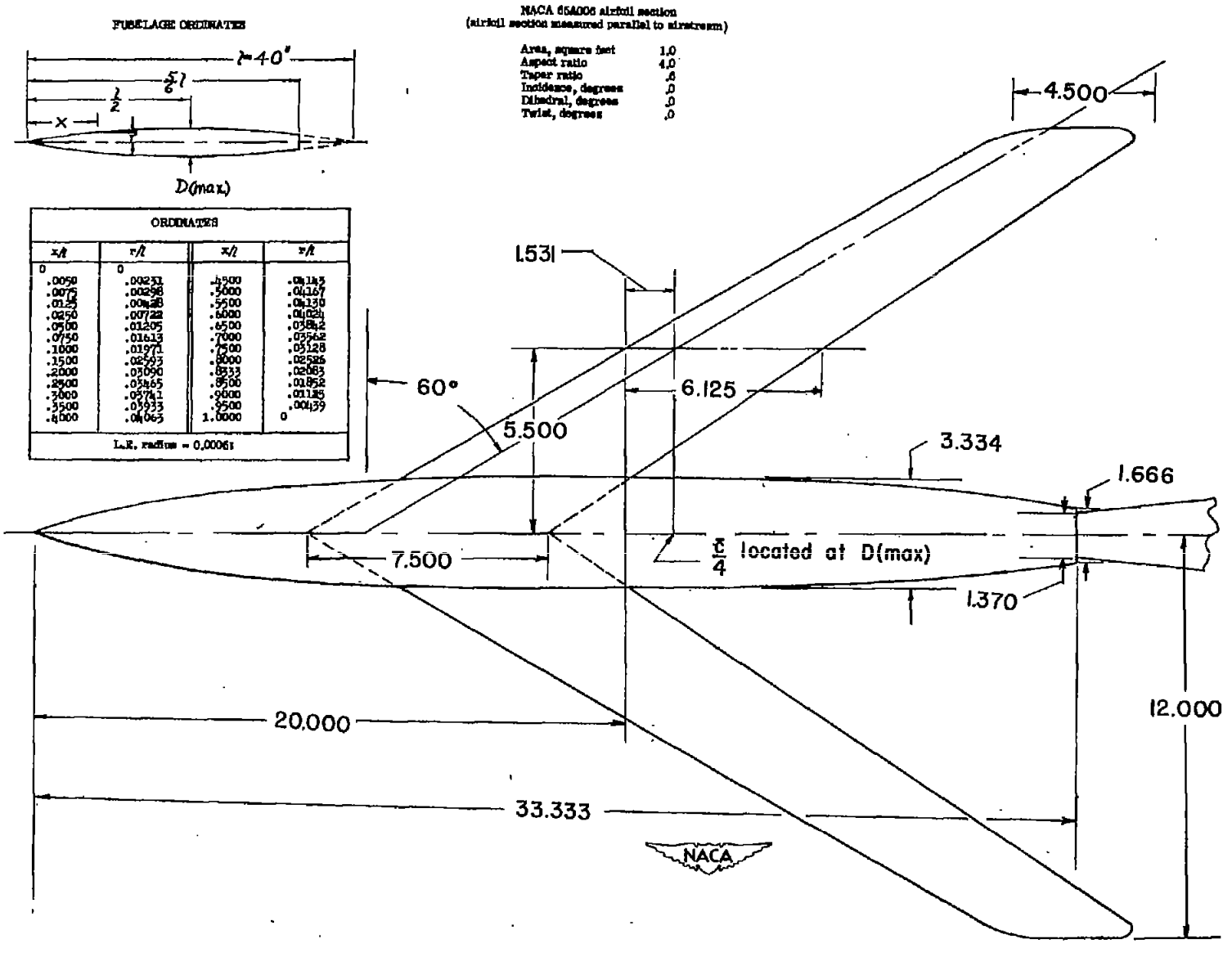

Figure 1.- Sketch of wing-fuselage combination. All dimensions are in inches unless otherwise noted.

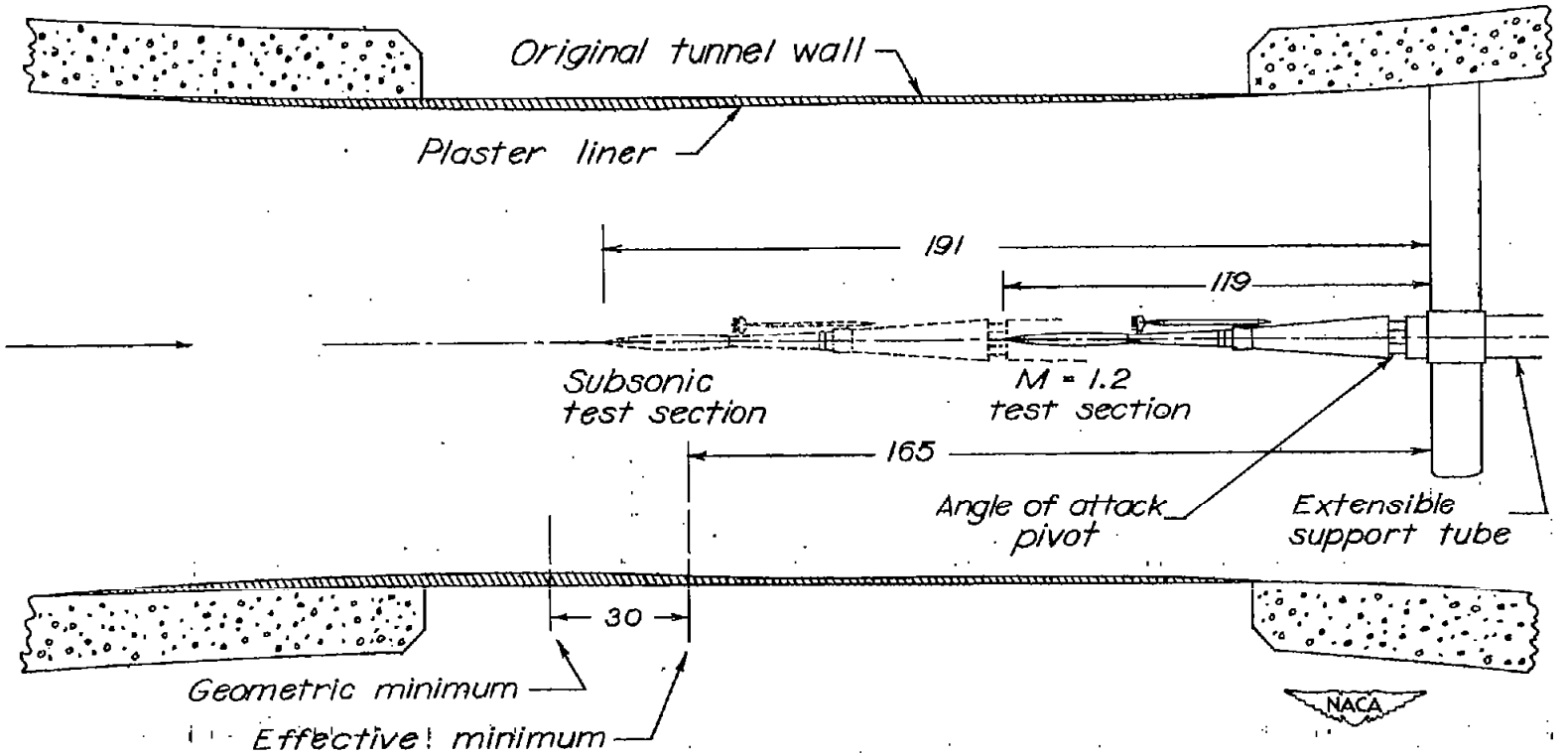

Figure 2.- Drawing of model locations in the subsonic and supersonic test section of the Langley 8-foot high-speed tunnel. All dimensions are in inches.

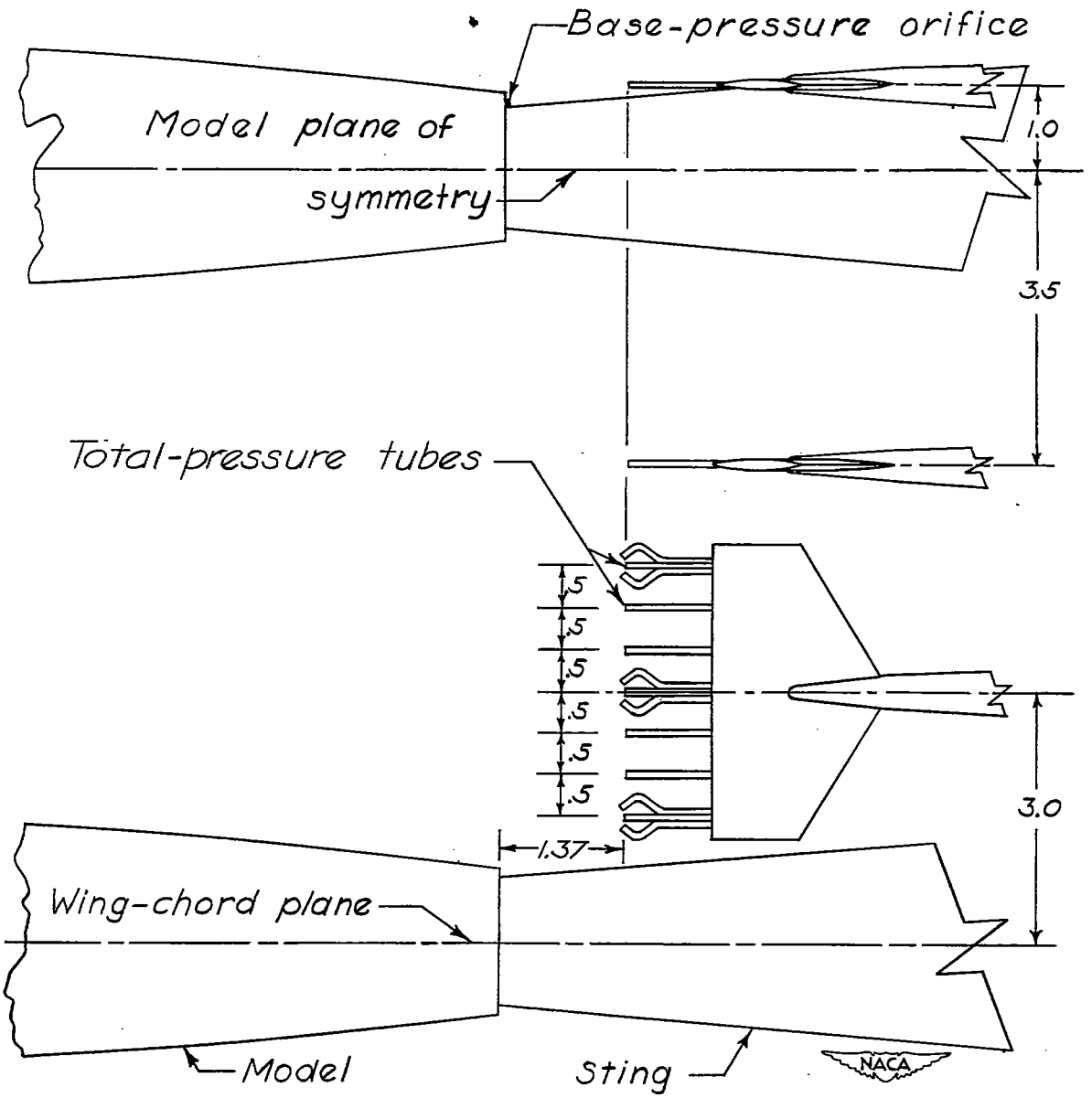

Figure 3.- Details of the rakes used for wake survey and downwash measurement. All dimensions are in inches.

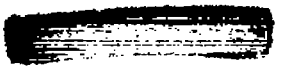

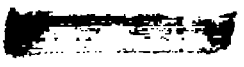

Figure 4.- Close-up photograph of the model installed on the sting-support system in the Langley 8-foot high-speed tunnel.

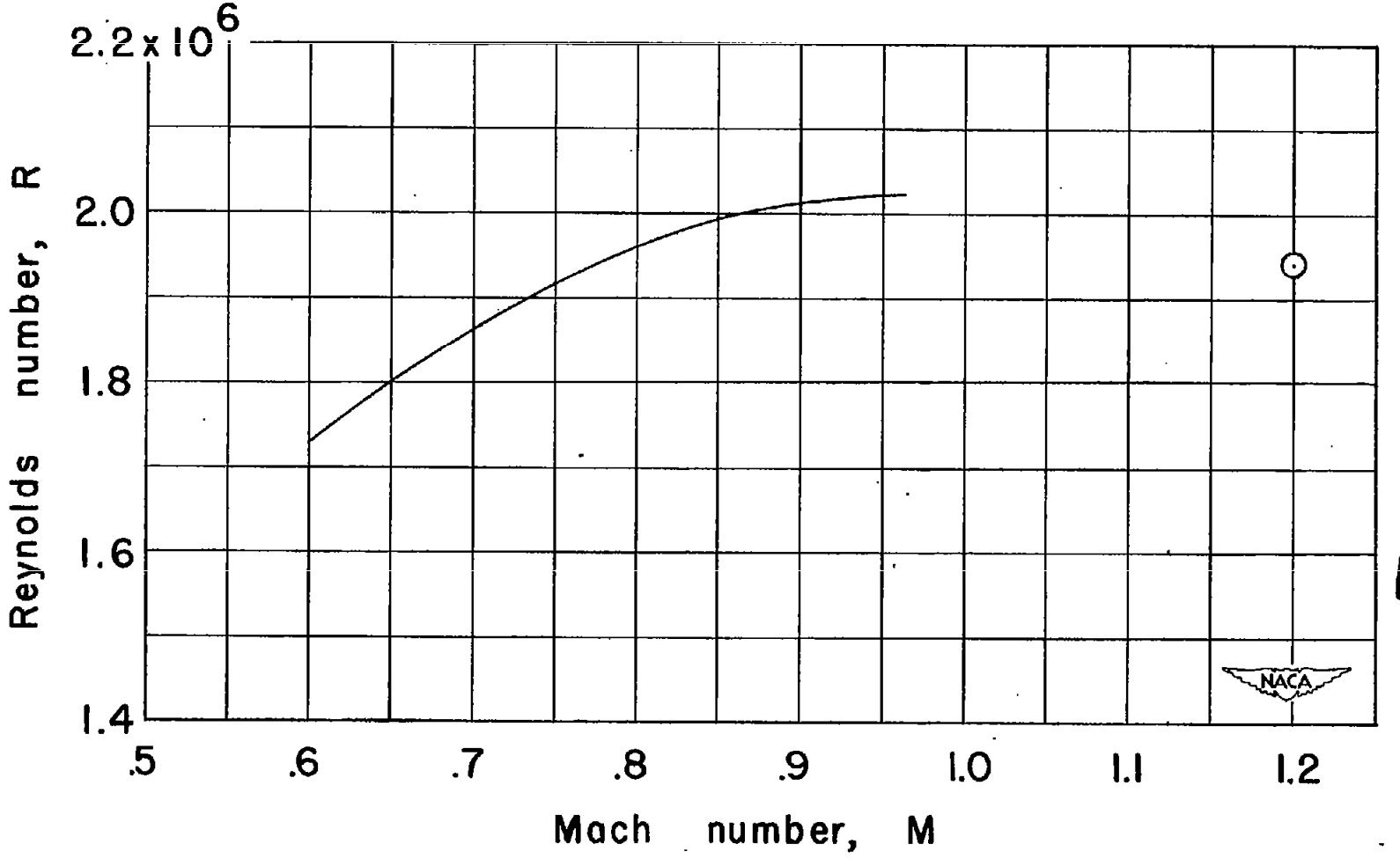

Figure 5.- Variation of test Reynolds number based on a $\bar{c}$ value of 0.51 feet with Mach number.

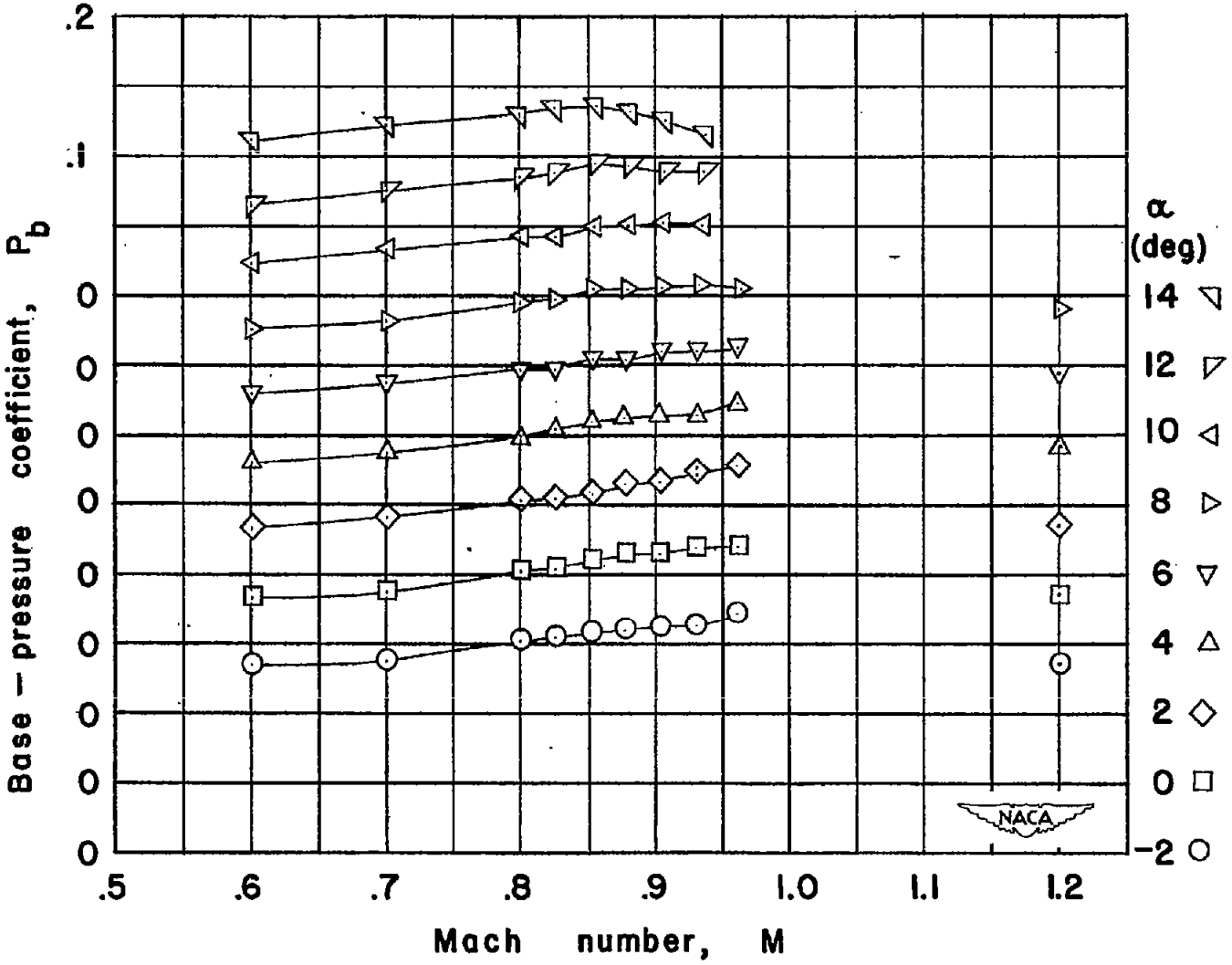

Figure 6.- Base-pressure coefficients for the wing-fuselage configuration for several angles of attack at various Mach numbers.

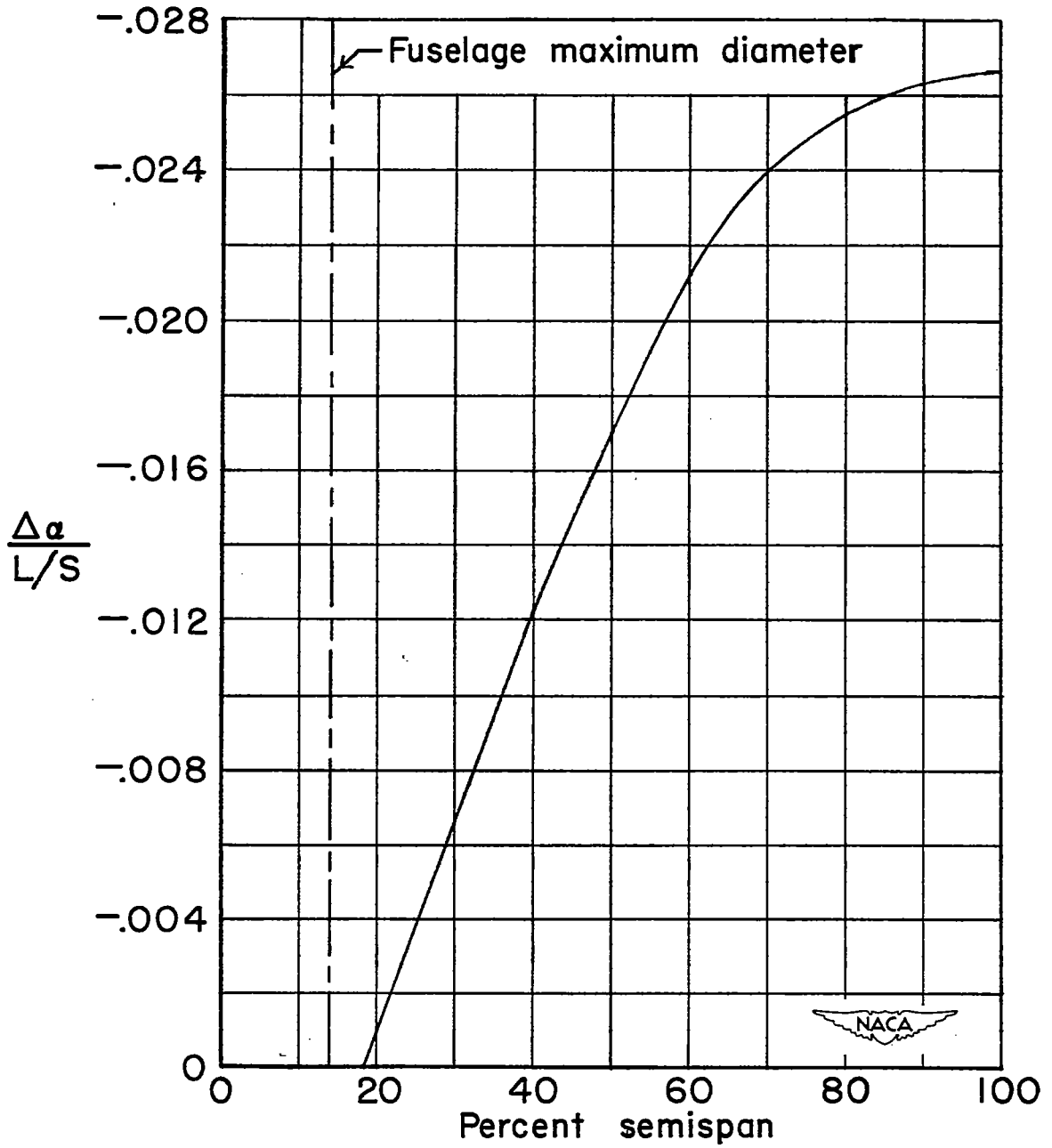

(a) Static test results.

Figure 7.- Effect of wing bending on a 60° sweptback aluminum wing with an NACA 65A006 airfoil section. A = 4; λ = 0.6.

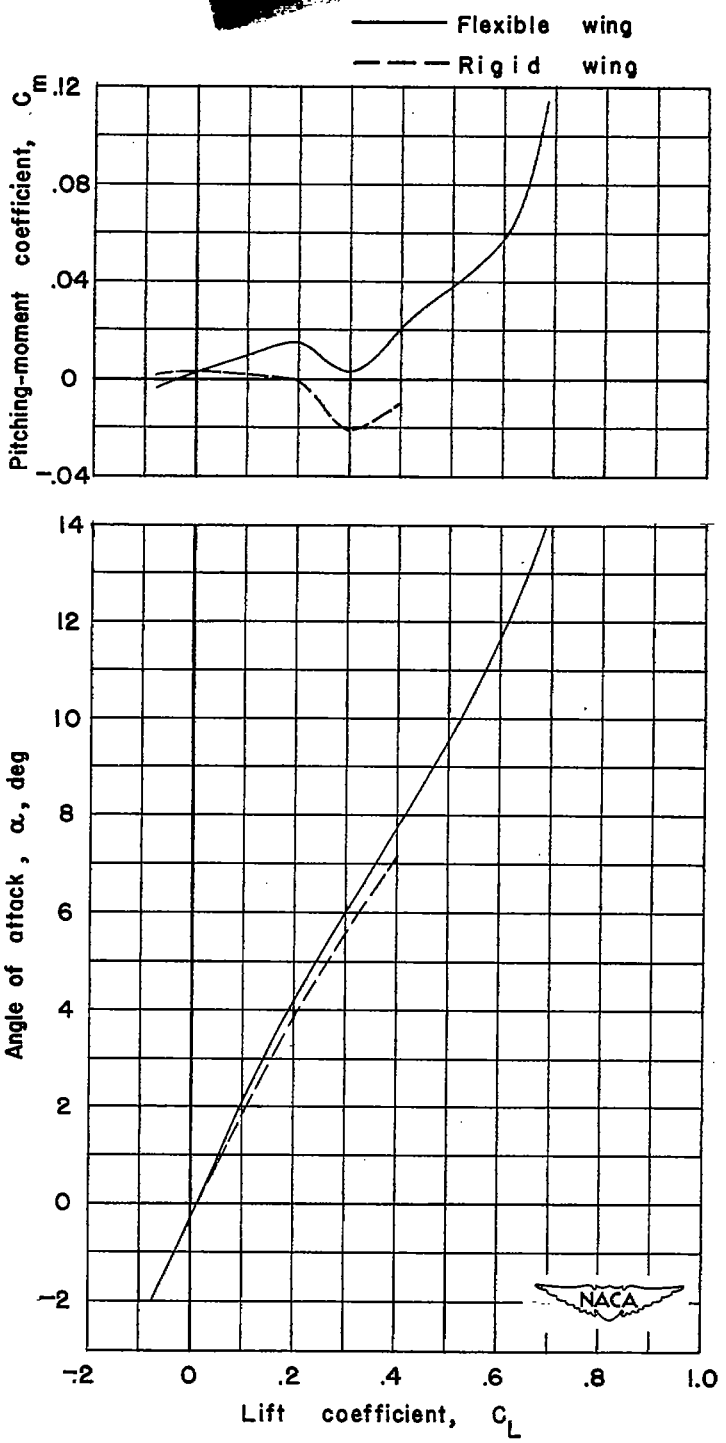

(b) Aerodynamic characteristics at M = 0.90.

Figure 7.- Concluded.

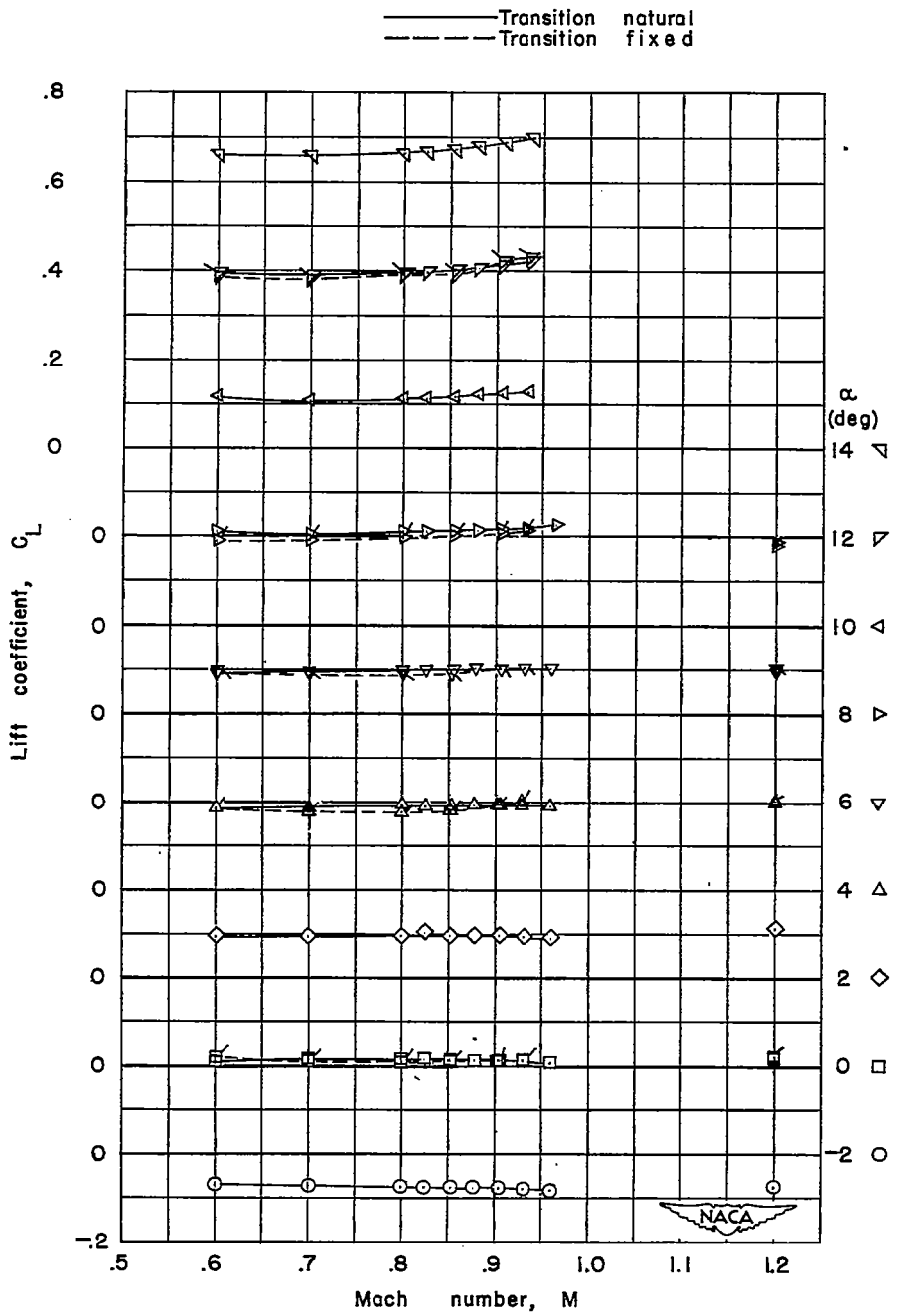

(a) Lift.

Figure 8.- Variation of the aerodynamic characteristics with Mach number for various angles of attack of the wing-fuselage configuration. The effect of a transition strip placed at the 10-percent wing chord and on the fuselage approximately 10 percent from the nose is indicated by flagged symbols.

[redacted]

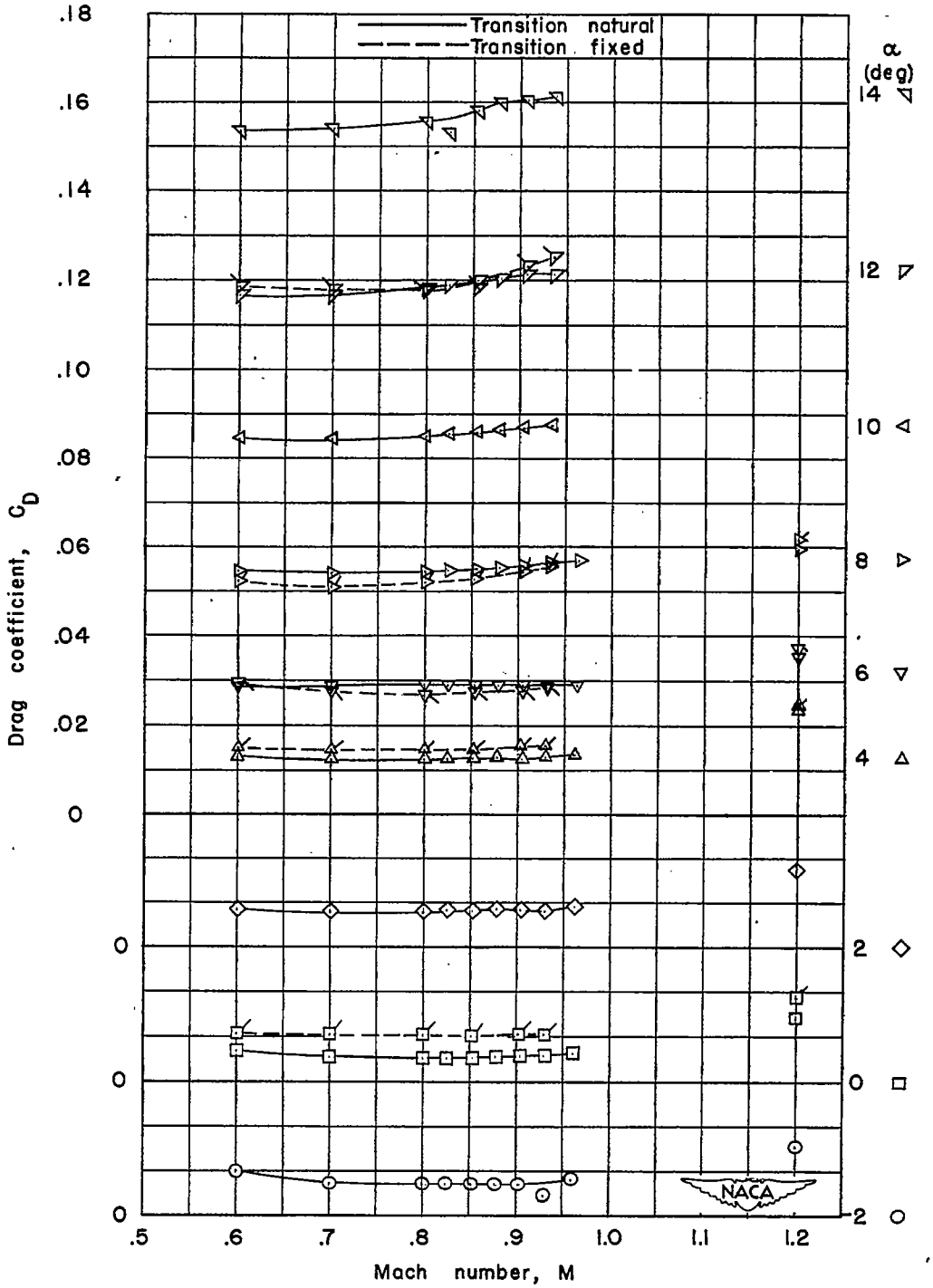

(b) Drag.

Figure 8.- Continued.

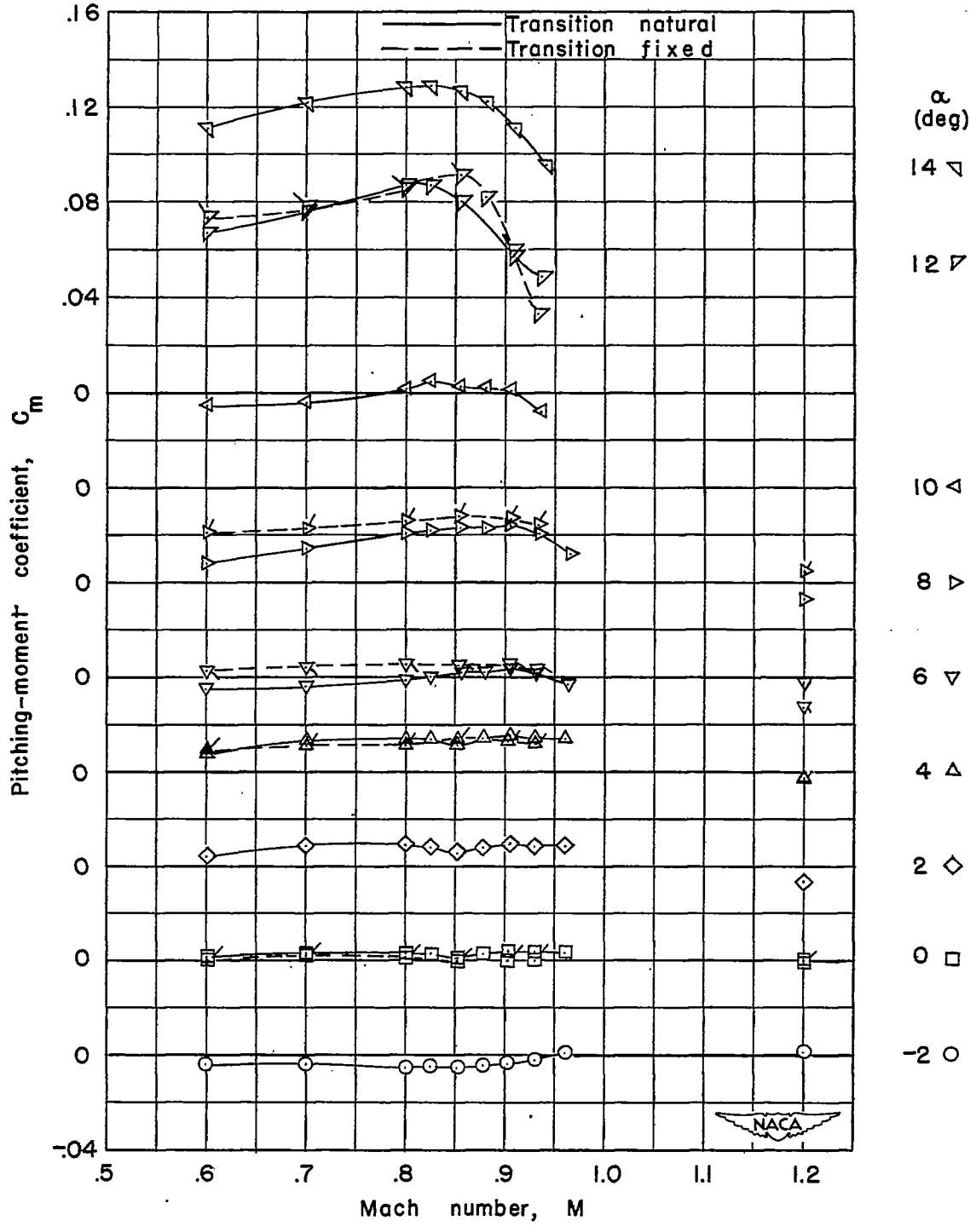

(c) Pitching moment.

Figure 8.- Concluded.

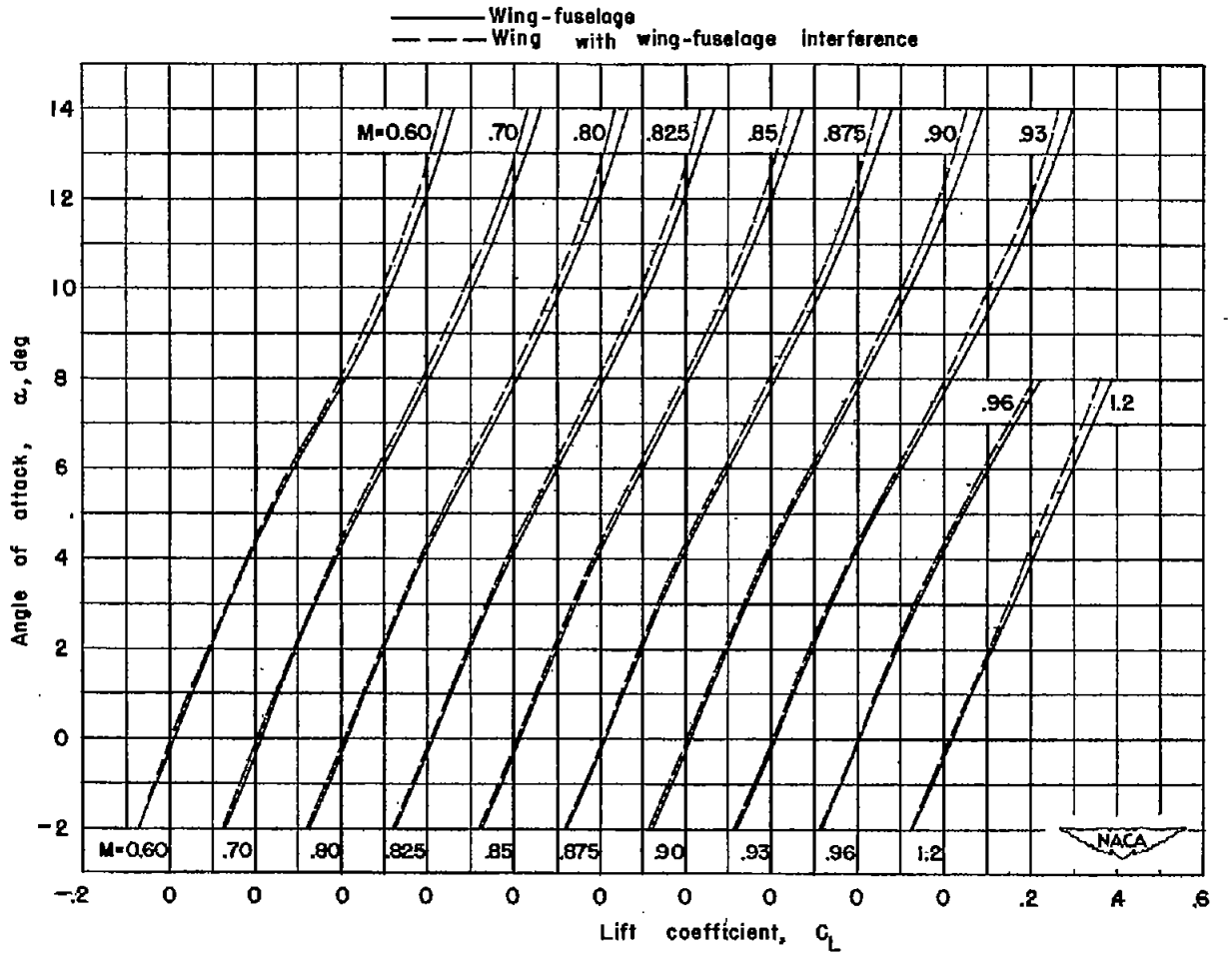

(a) Angle-of-attack characteristics.

Figure 9.- Variation of the aerodynamic characteristics with lift coefficient for the wing-fuselage configuration and the wing with wing-fuselage interference at various Mach numbers.

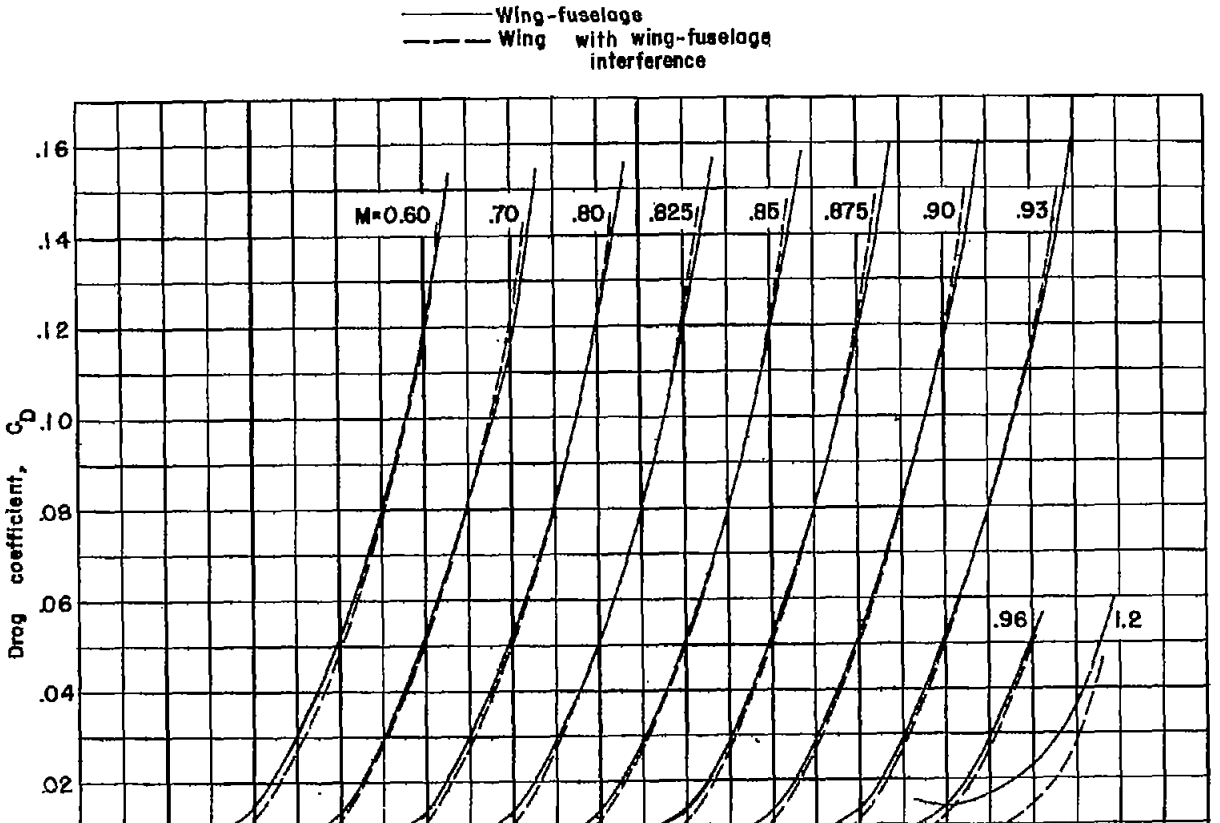

(b) Drag characteristics.

Figure 9.- Continued.

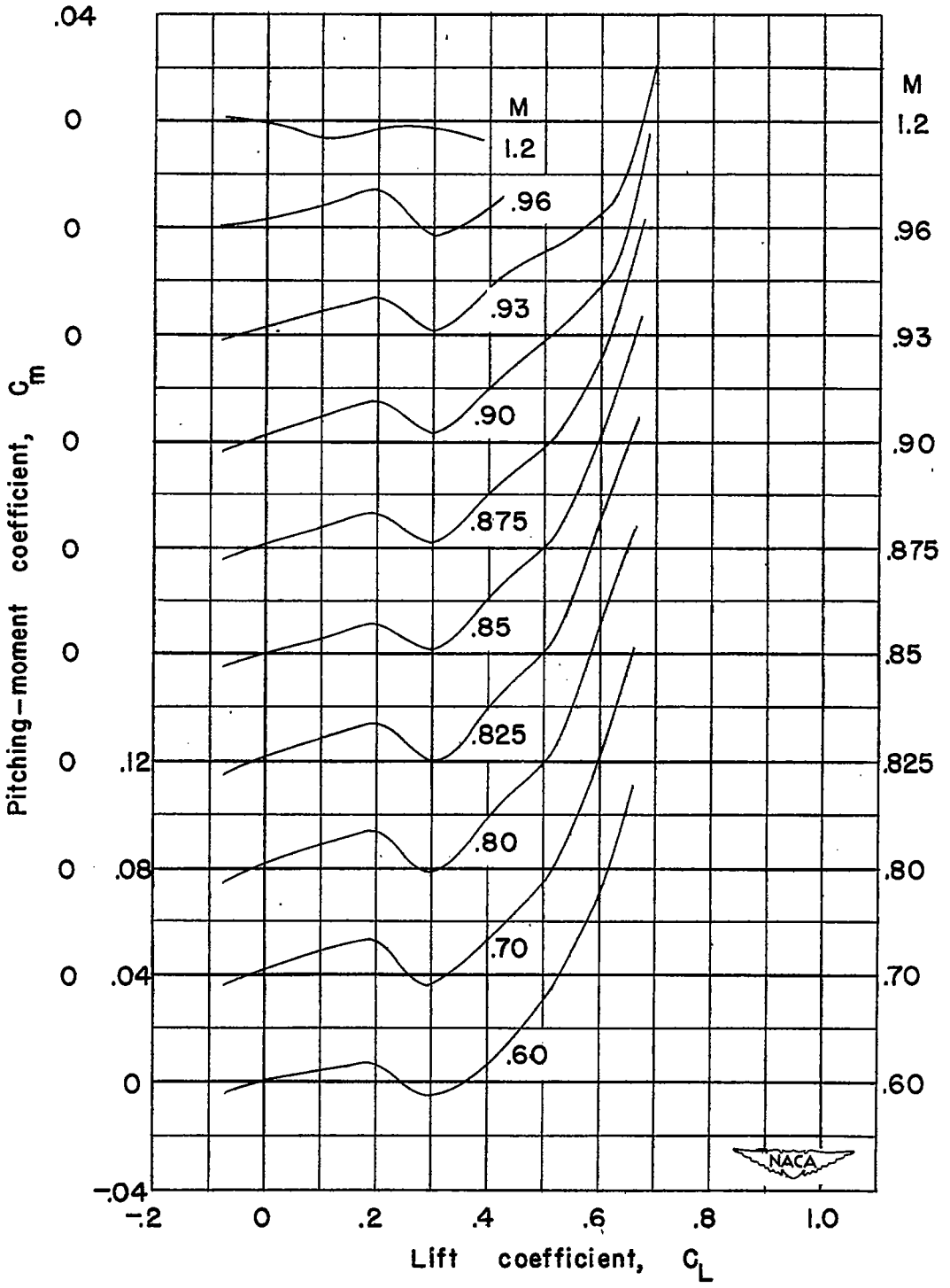

(c) Pitching-moment characteristics (wing fuselage).

Figure 9.- Continued.

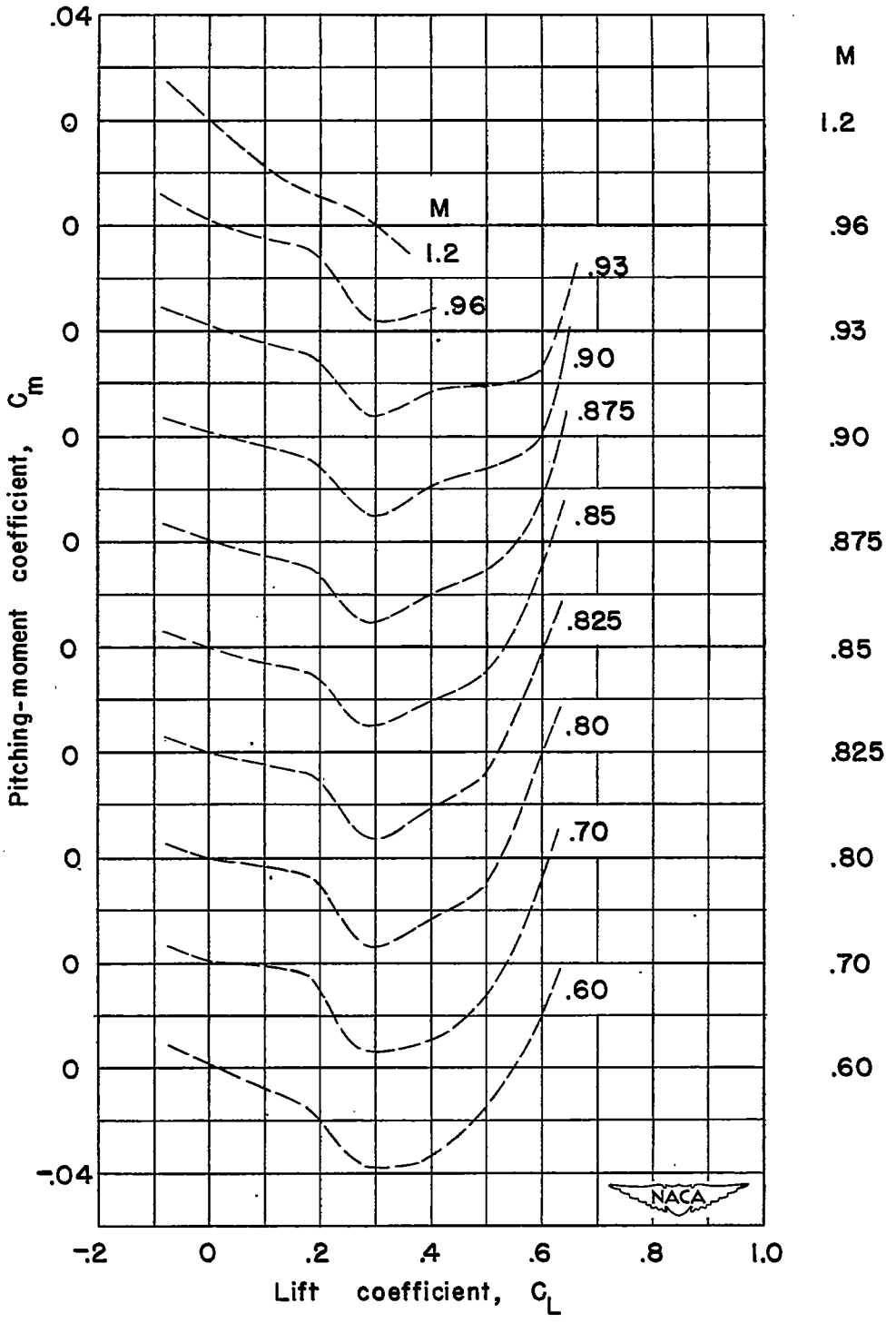

(d) Pitching-moment characteristics (wing with wing-fuselage interference).

Figure 9.- Concluded.

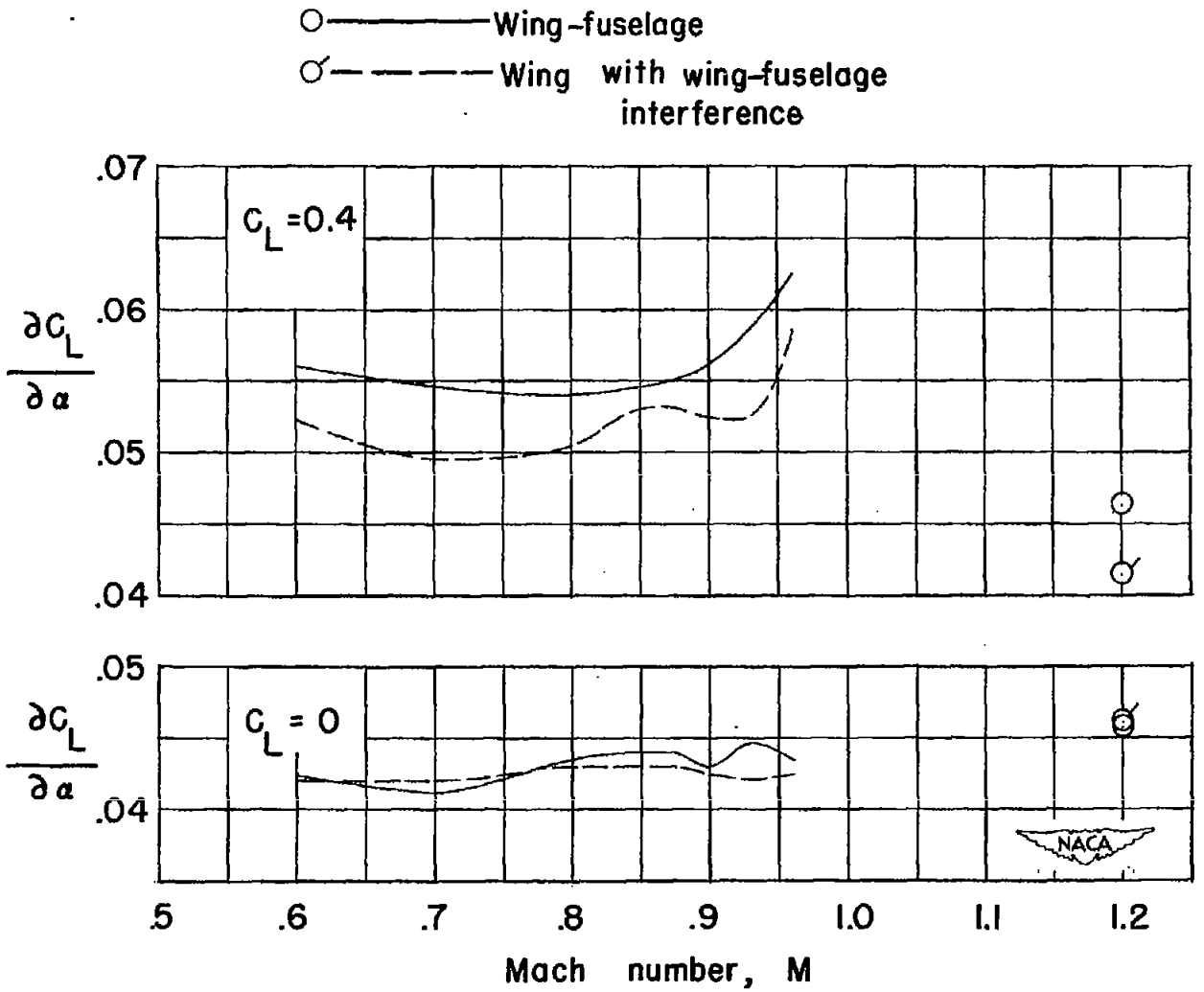

Figure 10.- Comparison of the slopes of the lift curve (at $C_L = 0$ and $C_L = 0.4$) with Mach number for the wing-fuselage configuration and the wing with wing-fuselage interference.

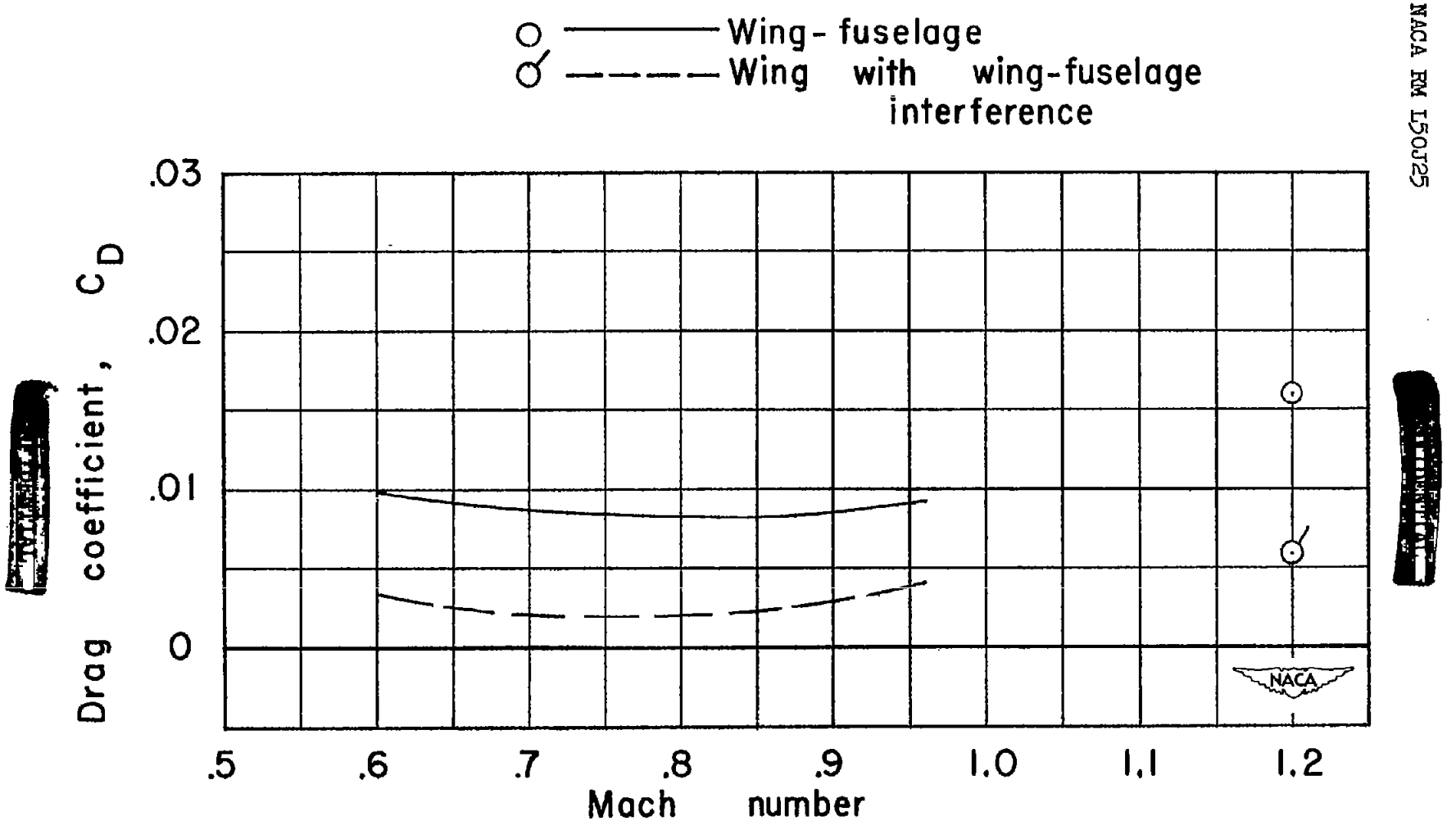

Figure 11.- Comparison of the drag coefficients at zero lift with Mach number for the wing-fuselage configuration and the wing with wing-fuselage interference. Sting-interference tares have been applied to the wing-fuselage-configuration data.

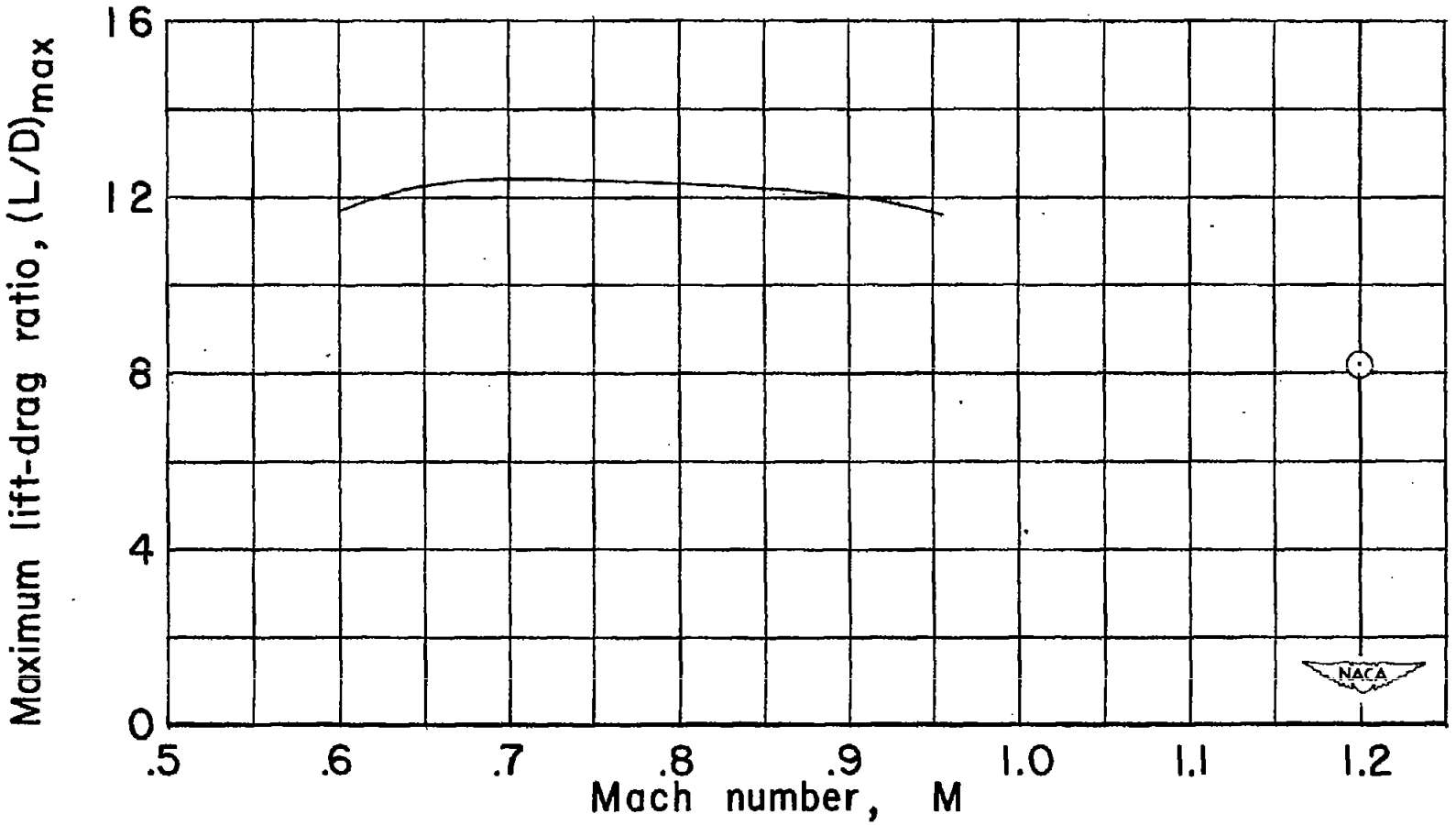

Figure 12.- Variation of the maximum lift-drag ratio with Mach number for the wing-fuselage configuration. Sting-interference tares have been applied to the data.

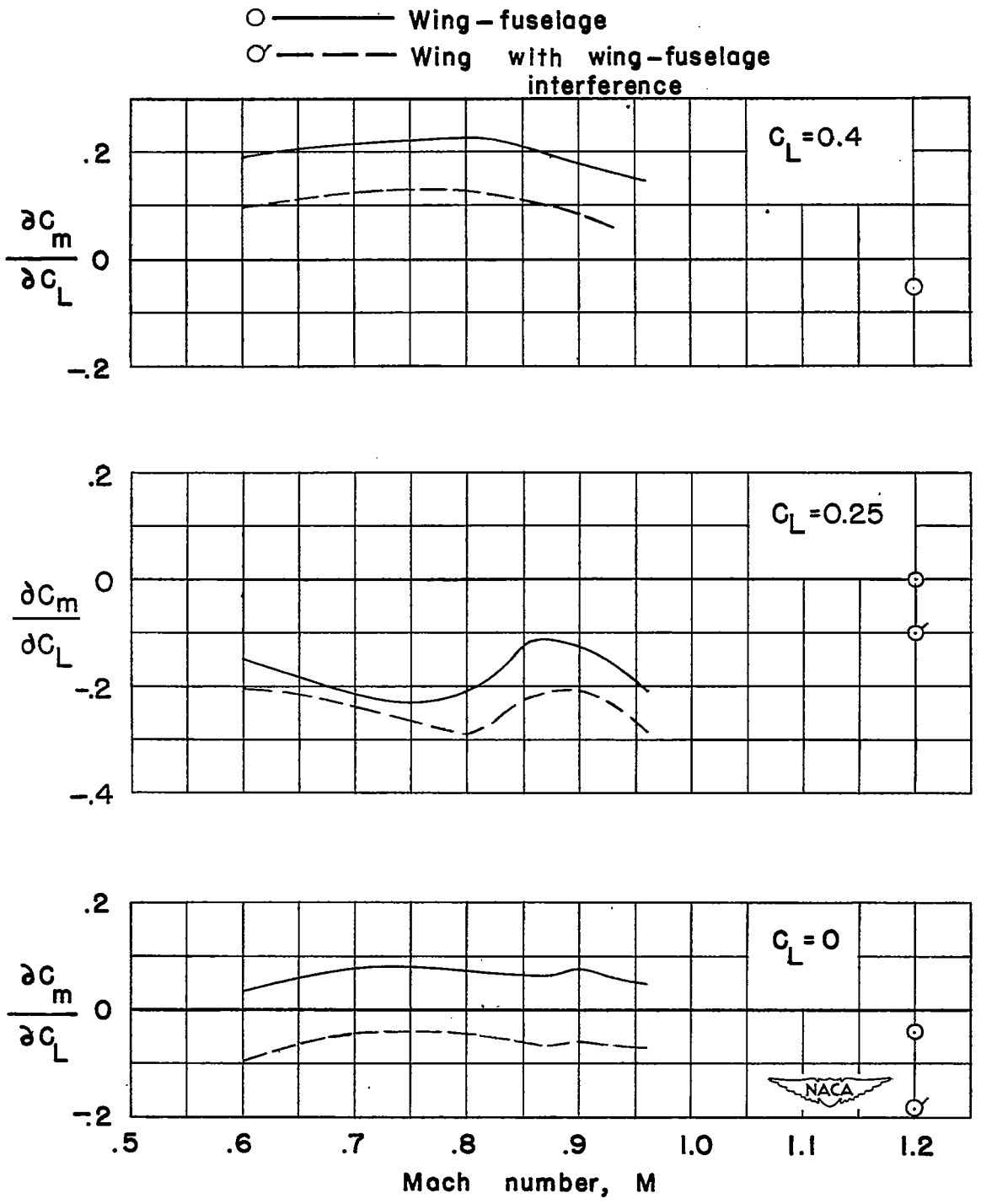

Figure 13.- Variation of the slopes of the pitching-moment curve with Mach number for the wing-fuselage configuration and the wing with wing-fuselage interference at several lift coefficients (C_L = 0, 0.25, and 0.4).

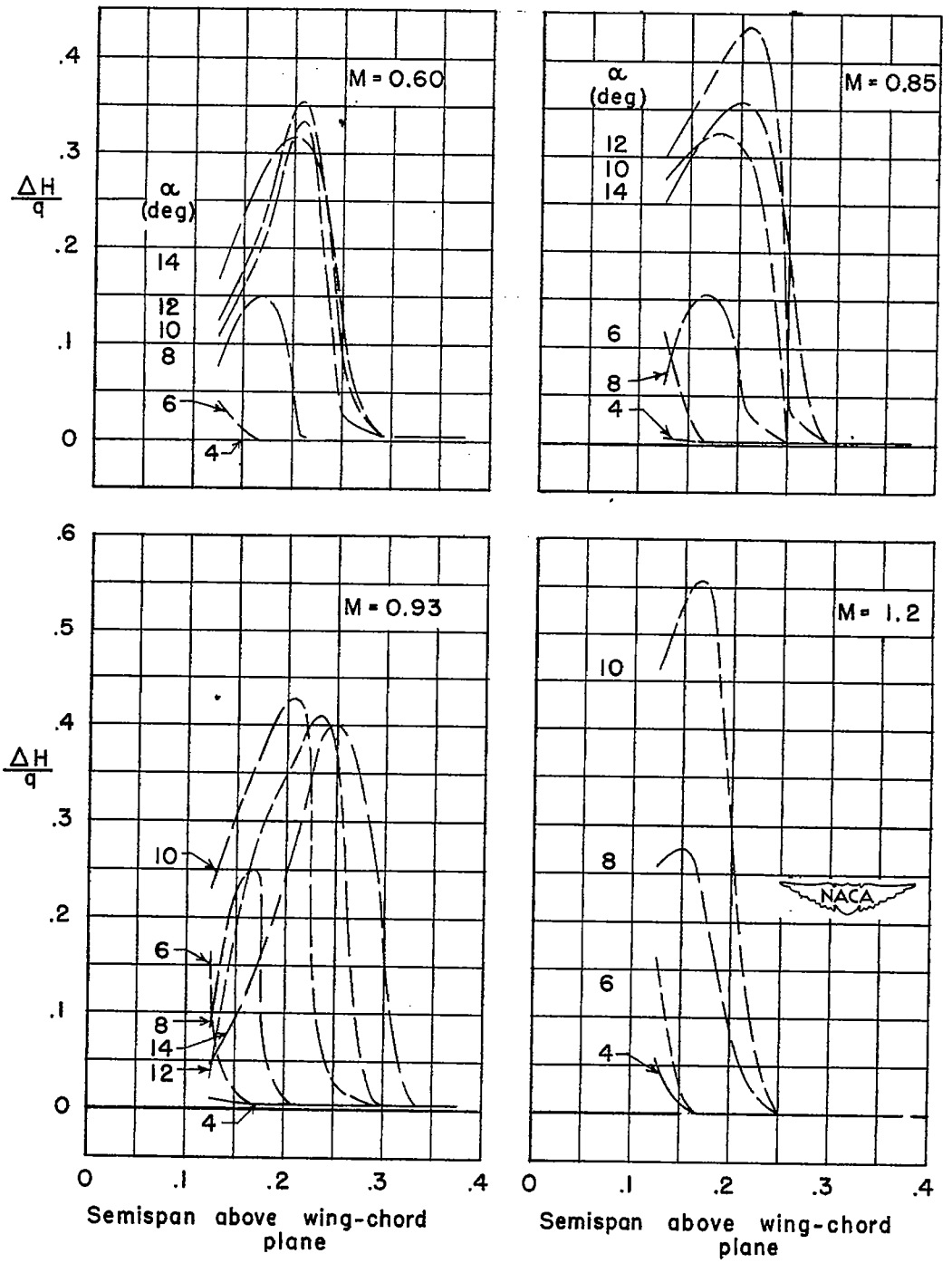

(a) Location 0.083 semispan from plane of symmetry.

Figure 14.- Wake characteristics as measured 1.225 wing semispans behind the 0.25 $\bar{c}$ position of the wing.

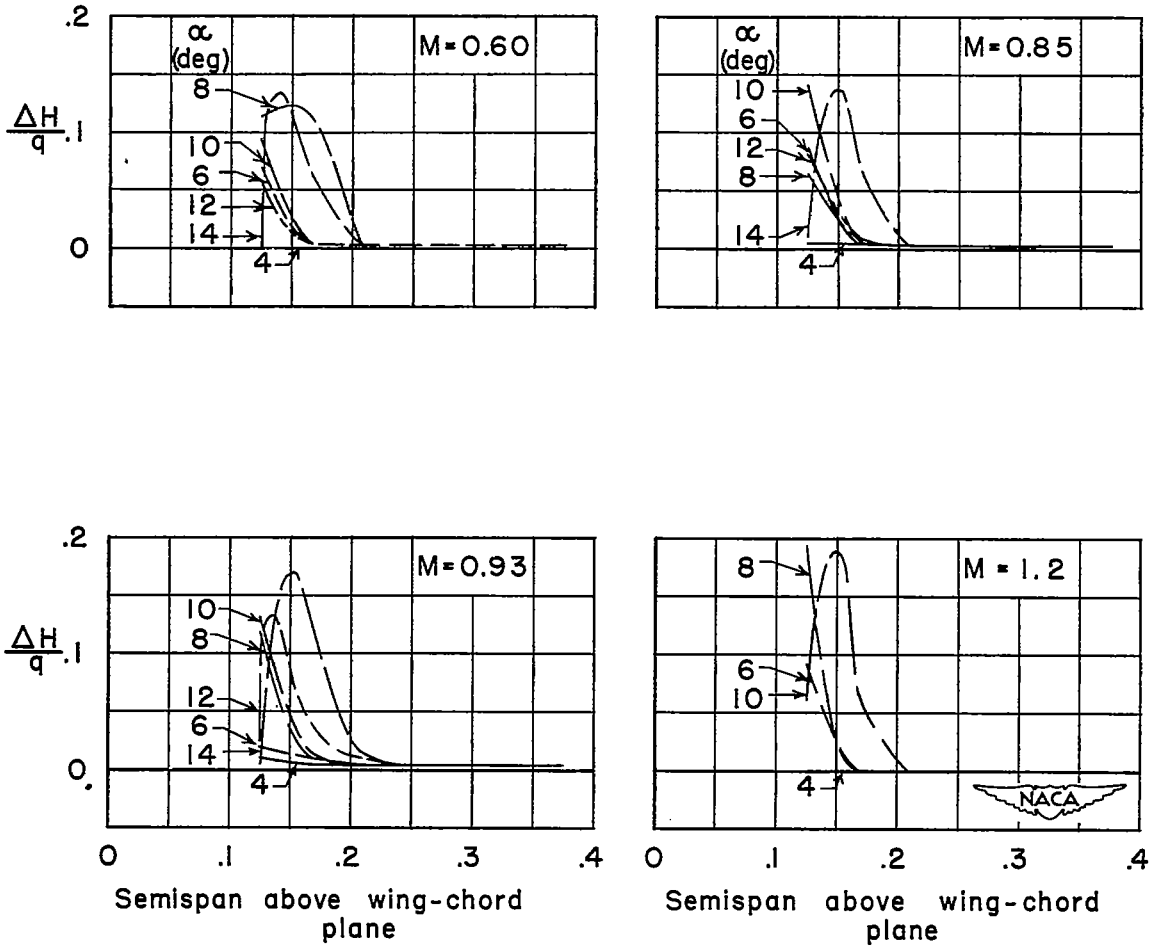

(b) Location 0.292 semispan from plane of symmetry.

Figure 14.- Concluded.

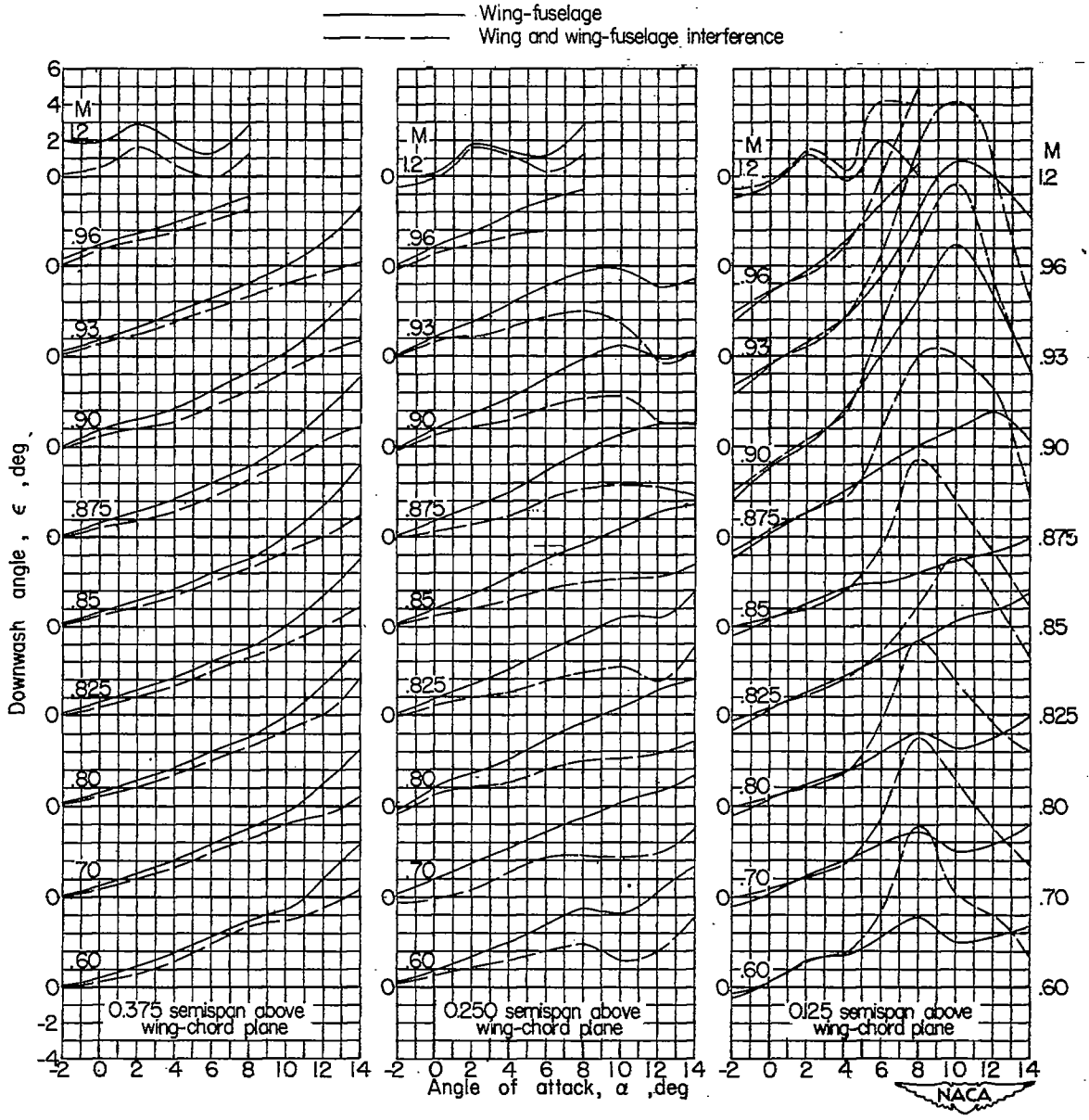

(a) Location 0.083 semispan from plane of symmetry.

Figure 15.- Variation of downwash angle with wing angle of attack for various Mach numbers at three tail locations as measured 1.225 wing semispans behind the 0.25$\bar{c}$ position of the wing.

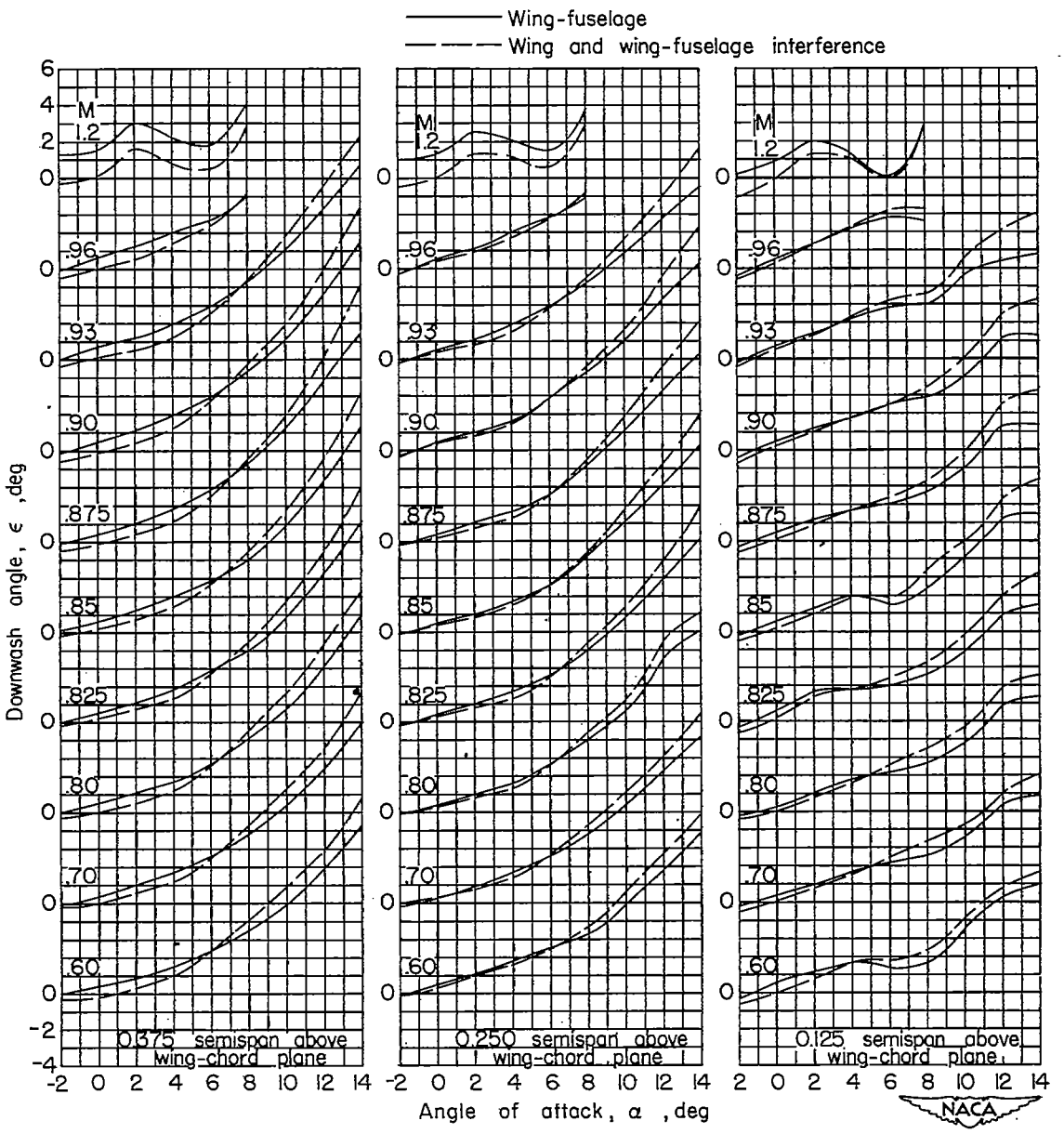

(b) Location 0.292 semispan from plane of symmetry.

Figure 15.- Concluded.

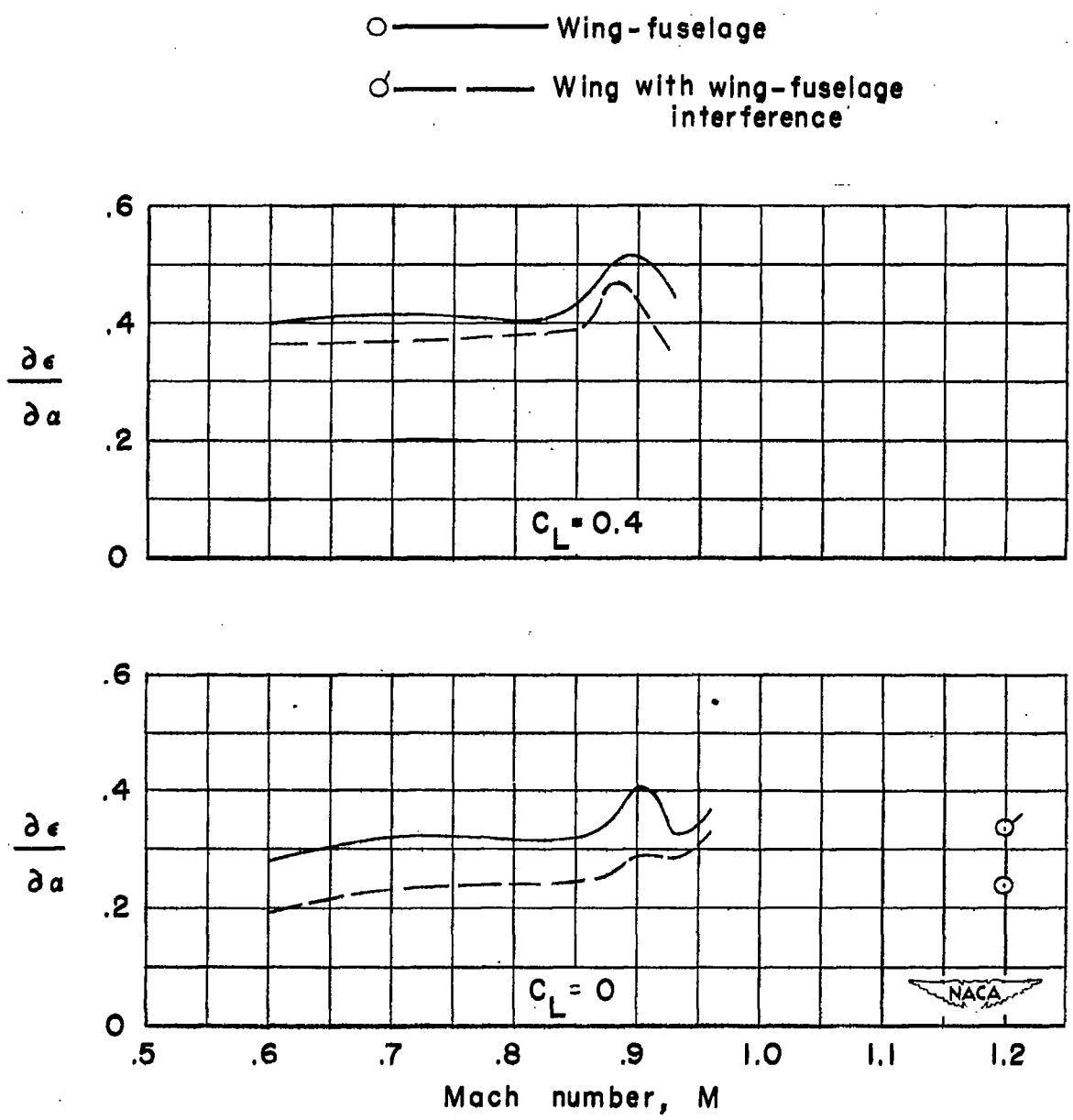

(a) Location 0.083 semispan from plane of symmetry.

Figure 16.- Variation of the slope of the downwash curve with Mach number at two lift coefficients for a probable tail location at two wing semispan positions at a tail height of 0.375 wing semispans above the wing-chord plane.

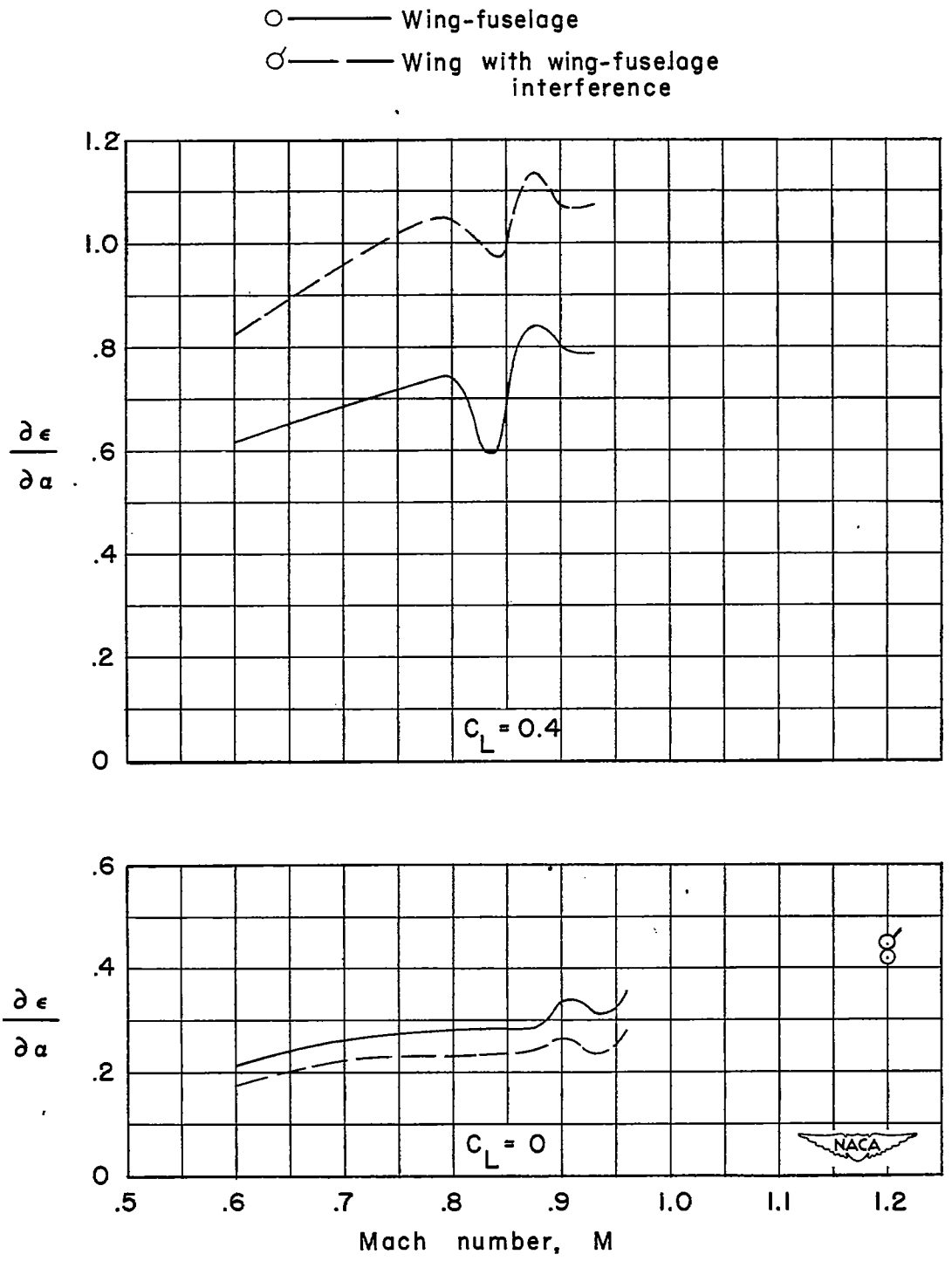

(b) Location 0.292 semispan from plane of symmetry.

Figure 16.- Concluded.

[redacted]